

Georgia State University

ScholarWorks @ Georgia State University

Geosciences Theses

Department of Geosciences

8-12-2016

The Evaluation of Measuring Stream Channel Morphology using Unmanned Aerial System-Based Structure-From-Motion Photogrammetry

William Ballow

Follow this and additional works at: https://scholarworks.gsu.edu/geosciences_theses

Recommended Citation

Ballow, William, "The Evaluation of Measuring Stream Channel Morphology using Unmanned Aerial System-Based Structure-From-Motion Photogrammetry." Thesis, Georgia State University, 2016.
doi: <https://doi.org/10.57709/8692577>

This Thesis is brought to you for free and open access by the Department of Geosciences at ScholarWorks @ Georgia State University. It has been accepted for inclusion in Geosciences Theses by an authorized administrator of ScholarWorks @ Georgia State University. For more information, please contact scholarworks@gsu.edu.

THE EVALUATION OF MEASURING STREAM CHANNEL MORPHOLOGY USING
UNMANNED AERIAL SYSTEM-BASED STRUCTURE-FROM-MOTION
PHOTOGRAMMETRY

by

WILLIAM BALLOW

Under the Direction of Katie Price, PhD

ABSTRACT

As part of a collaborative project at a stream segment reach on Proctor Creek in Atlanta, GA, UAV-based SfM photogrammetry was tested as a method for collecting fluvial topographic data relative to traditional USGS total station surveying methods. According to the USGS method, 11 transects were surveyed, and imagery was collected via a UAV to create a SfM DEM. The resulting DEM was incomplete but showed promise for the SfM method. Two additional stream segments were chosen in the Atlanta area, the first along SFPC in DHCL and the second along NFPC near Buford Hwy. For each site 11 transects were surveyed along with submerged GCPs so that the SfM DEMs could be compared to the surveyed data. The BW and BD values were collected from the TS transects and the DEM transects and compared according to the percent difference between the two. For SFPC, the average percent difference values for

BW and BD were, respectively, 15.9 and 26.0 with standard deviations of 15.7 and 18.0. For NFPC, the BW and BD average percent difference values were 6.8 and 7.5 with standard deviations of 3.9 and 5.9. The GCPs were also compared for each site using linear regressions. There was no strong correlation for SFPC ($R^2 = 0.31$ and $p\text{-value} > 0.05$), but there was a strong relationship indicated for NFPC ($R^2 = 0.78$ and $p\text{-value} < 0.05$). While the results of this study are variable, the results do indicate promise for future work on this emerging method.

INDEX WORDS: structure from motion, unmanned aerial system, photogrammetry, digital elevation model, fluvial, geomorphology

THE EVALUATION OF MEASURING STREAM CHANNEL MORPHOLOGY USING
UNMANNED AERIAL SYSTEM-BASED STRUCTURE-FROM-MOTION
PHOTOGRAMMETRY

by

WILLIAM BALLOW

A Thesis Submitted in Partial Fulfillment of the Requirements for the Degree of

Master of Science

in the College of Arts and Sciences

Georgia State University

2016

Copyright by
William Bradford Ballow
2016

THE EVALUATION OF MEASURING STREAM CHANNEL MORPHOLOGY USING
UNMANNED AERIAL SYSTEM-BASED STRUCTURE-FROM-MOTION
PHOTOGRAMMETRY

by

WILLIAM BALLOW

Committee Chair: Katie Price

Committee: Daniel Deocampo

Brian Meyer

Electronic Version Approved:

Office of Graduate Studies

College of Arts and Sciences

Georgia State University

June 2016

ACKNOWLEDGEMENTS

This study, and all of my work as a graduate student at Georgia State University, would not have been possible if it were not for the entire staff and faculty of the Department of Geosciences. Every professor and lecturer that I have interacted with has been a huge part in my continued geoscience education. With classes such as Advanced GIS with Dr. Dai, Environmental Instrumentation with Dr. Kabengi, and Geoinformatics with Dr. Babaie, my coursework has been diverse and will therefore benefit me for years to come. In addition to what I have gained from the department academically, the department's staff has helped make this possible by being available and knowledgeable when I needed assistance with computer software, course registration, and finances.

My committee members, Dr. Deocampo and Dr. Meyer, deserve special thanks for taking the time to be a part of this work. They have both been excellent teachers to me, which makes their input particularly meaningful. Similarly, the input of my thesis advisor, Dr. Katie Price, has been the foundation of my work at GSU. But, of course, my appreciation of her help goes far beyond that. She has been an invaluable and knowledgeable mentor, an excellent partner in the field, and a patient advisor. Some of the work done for this study was unfamiliar to both Dr. Price and me. Because of her abilities as a patient problem solver, I cannot imagine doing this work with anyone else.

This study initially started as a collaborative effort of interested seminar students led by Dr. Price. Eli Koslofsky, Elinor Sattler, Jesse Hughes, Tina Mehaffey, Jeff Riley, and Devin Thiery all made this work possible and helped develop some of the methods used for this study. Furthermore, we had the help of the GSU Library CURVE staff aid us in our initial efforts. Robert Bryant introduced us to SfM software, Joseph Hurley helped us access CURVE as

needed, and Andrew Vaughan not only proved to be a great drone pilot and drone instructor, but he also continued to patiently help me with my work involving SfM software. Lastly, I must thank my wife, Julia Ballow. She has supported me in every way possible, and I truly do not know where I would be without her. More than that, she also came to help Dr. Price and me with fieldwork on two separate occasions. Any wife that keeps a smile all day after getting Peachtree Creek water in her waders at 8am, and in January, is a truly special partner.

TABLE OF CONTENTS

ACKNOWLEDGEMENTS	v
LIST OF TABLES	ix
LIST OF FIGURES	x
LIST OF ABBREVIATIONS	xii
1 INTRODUCTION	1
1.1 Existing Methods	1
<i>1.1.1 Total Stations and Ground Survey Methods</i>	<i>2</i>
<i>1.1.2 Laser Scanning</i>	<i>4</i>
<i>1.1.3 Digital Photogrammetry</i>	<i>5</i>
<i>1.1.4 UAS and SfM-photogrammetry.....</i>	<i>6</i>
1.2 Study Overview	8
<i>1.2.1 Site Locations</i>	<i>9</i>
<i>1.2.2 Study Purpose and Significance.....</i>	<i>13</i>
2 Methods	15
2.1 Total Station Transects.....	15
2.2 Control Points.....	15
2.3 Image Acquisition.....	16
2.4 Image Selection.....	17
2.5 SfM Processing	18

2.6	Quantitative Topographic Data Comparison	22
3	RESULTS	23
3.1	SfM Processing	23
3.1.1	<i>Proctor Creek</i>	23
3.1.2	<i>South Fork Peavine Creek</i>	26
3.1.3	<i>North Fork Peachtree Creek</i>	30
3.2	Transects and DEMs	33
3.2.1	<i>Proctor Creek</i>	33
3.2.2	<i>South Fork Peavine Creek</i>	36
3.2.3	<i>North Fork Peachtree Creek</i>	38
3.3	Quantitative Topographic Data Comparison	40
3.3.1	<i>South Fork Peavine Creek</i>	40
3.3.2	<i>North Fork Peachtree Creek</i>	42
4	Discussion.....	44
4.1	Considerations for Future Work	45
5	CONCLUSIONS	49
	REFERENCES.....	51

LIST OF TABLES

Table 3-1: TS and DEM BW and BD values for SFPC, as well as the percent difference between these values	41
Table 3-2: TS and DEM BW and BD values for NFPC, as well as the percent difference between these values	43

LIST OF FIGURES

Figure 1.1: Example of the USGS-NAWQA survey method for a wadeable stream.....	3
Figure 1.2: Study area on Proctor Creek in Fulton County	10
Figure 1.3: Study area on South Fork Peavine Creek in DeKalb County, Georgia.....	11
Figure 1.4: Study area on NFPC in DeKalb County, Georgia.....	12
Figure 2.1: Image taken during flight at the DHGC site location showing the GCPs placed along the reach banks and in the stream bed	16
Figure 2.2: DJI Phantom II with a 10 MP GoPro camera attached to a Zenmuse 3-axis gimbal.	17
Figure 2.3: Images of the SFPC dense point cloud.....	20
Figure 2.4: Images of the NFPC dense point cloud.....	21
Figure 3.1: SfM model of the upstream chunk at Proctor Creek also showing GCPs.....	24
Figure 3.2: Examples of drone-based aerial imagery of the Proctor Creek study area	25
Figure 3.3: Locations where images were taken shown with image overlap statistics for the upstream chunk at Proctor Creek.....	26
Figure 3.4: SfM model of the SFPC stream segment showing the locations of GCPs used as spatial reference	27
Figure 3.5: Example of drone-based imagery of SFPC. The top photo was not ultimately used in the generation of the model and DEM.....	28
Figure 3.6: Locations where images were taken shown with image overlap statistics for SFPC.	29
Figure 3.7: SfM model of the SFPC stream segment showing the locations of GCPs used as spatial reference	30
Figure 3.8: Example of drone-based imagery of NFPC. Both photos were used in model generation.....	31

Figure 3.9: Locations where images were taken shown with image overlap statistics for SFPC.	32
Figure 3.10: Proctor Creek at Pet Heaven. SfM-derived DEM shown with TS transect start and end points as well as DEM transect locations.....	34
Figure 3.11: Proctor Creek DEM and TS transects plotted atop one another.....	35
Figure 3.12: South Fork Peavine Creek at DHGC. SfM-derived DEM shown with TS points as well as DEM transect locations.....	36
Figure 3.13: SFPC DEM and TS transects plotted atop one another.....	37
Figure 3.14: North Fork Peachtree Creek SfM-derived DEM shown with TS points as well as DEM transect locations.....	38
Figure 3.15: NFPC DEM and TS transects plotted atop one another.....	39
Figure 3.16: Scatter plot and simple linear regression with corresponding SFPC TS and DEM control point z values plotted against one another.....	41
Figure 3.17: Scatter plot and simple linear regression with corresponding NFPC TS and DEM control point z values plotted against one another.....	43
Figure 3.18: Example of Photoscan premade targets for GCP use.....	46

LIST OF ABBREVIATIONS

3D.....	Three-dimensional
ALS.. ..	Aerial Laser Scanner
BD.. ..	Bankfull Depth
GSU.. ..	Georgia State University
BW.. ..	Bankfull Width
CURVE... ..	Collaborative University Research & Visualization Environment
DEM.. ..	Digital Elevation Model
DHGC.. ..	Druid Hills Golf Course
EPA.. ..	Environmental Protection Agency
EXIF.. ..	Exchangeable Image File Format
LiDAR.. ..	Light Detection and Ranging
LS.. ..	Laser Scanner
MAS.. ..	Manned Aerial System
NFPC.. ..	North Fork Peachtree Creek
SfM.. ..	Structure-from-Motion
SFPC.. ..	South Fork Peavine Creek
TLS.. ..	Terrestrial Laser Scanner
TS.. ..	Total Station
UAS/UAV.. ..	Unmanned Aerial System/Vehicle
USGS.. ..	United States Geological Survey

1 INTRODUCTION

For the study of geomorphic processes, topographic data are essential, but these data do not always exist at high spatial and temporal resolutions (Bangen et al., 2014b; Fonstad et al., 2013; Wheaton et al., 2009; and Woodget et al., 2014). In the case of fluvial landforms, topographic data have a variety of applications, such as hydraulic modeling, sediment budget assessment, detecting geomorphic change, and habitat assessment (Marcus et al., 2012; Woodget et al. 2012). In general, there are three main sources of topographic data and across each type methodology, resolution, fiscal cost, and labor cost vary widely. Data can be generated via ground surveys, preexisting topographic maps, and remote sensing. When choosing a method, it is also important to consider whether or not the data are spatially continuous as well as the repeatability of the method, because when considering geomorphic change over time, repeat data must be collected for continuing studies (Bertin et al., 2015; Brasington et al., 2000; Clapuyt et al., 2015; Dietrich, 2015; Hicks, D.M., 2012; Ouédraogo et al., 2015; Wheaton et al. 2010).

1.1 Existing Methods

Total station surveying is one of the most commonly used ground survey methods for fluvial landforms, but remote sensing methods such as airborne laser scanning and photogrammetry have been evaluated for these landforms as well. However, recent advancements in software and image matching algorithms have possibly made structure-from-motion (SfM) photogrammetry a relatively cheap alternative data collection method. (Bertin et al., 2015; Brasington et al., 2000; Clapuyt et al., 2015; Dietrich, 2015; Hicks, 2012; Ouédraogo et al., 2015; Wheaton et al. 2010).

1.1.1 Total Stations and Ground Survey Methods

Traditional methods for gathering fluvial topographic data on wadeable streams typically rely on ground survey methods. These methods most often use tape measures, stadia rods, leveling equipment, global positioning systems (GPS), and total stations (TS) (Gregory and Calhoun, 2003; Fitzpatrick et al, 1998; Kang and Marston, 2006; Kaufmann et al., 1999; Woodget et al. 2014). Of these items, total stations are most reliable and accurate. However, the accuracy of total station-derived topographic data can be influenced by surveyor skill. Because total station surveying is a point-by-point method, surveyors may implement transect-based, grid-based, or topographically stratified methods for data collection (Bangen et al., 2014a; Beshr and Elnaga, 2011, Vallé and Pasternack, 2006). Both the United States Geological Survey (USGS) and the Environmental Protection Agency (EPA) use a transect-based method in stream surveys, but each of these approaches are time consuming and labor intensive. This limits the number of sites that can be surveyed and also reduces the frequency of sampling (Woodget et al., 2014; Fitzpatrick et al., 1998; Gregory and Calhoun, 2003; Kaufmann et al., 1999). For a given stream segment, the USGS-National Water Quality Assessment Program (NAWQA) method results in the production of 11 total station-derived transects that are spaced at intervals of two times the channel width (Fig. 1.1) (Fitzpatrick et al., 1998; Price and Leigh, 2006).

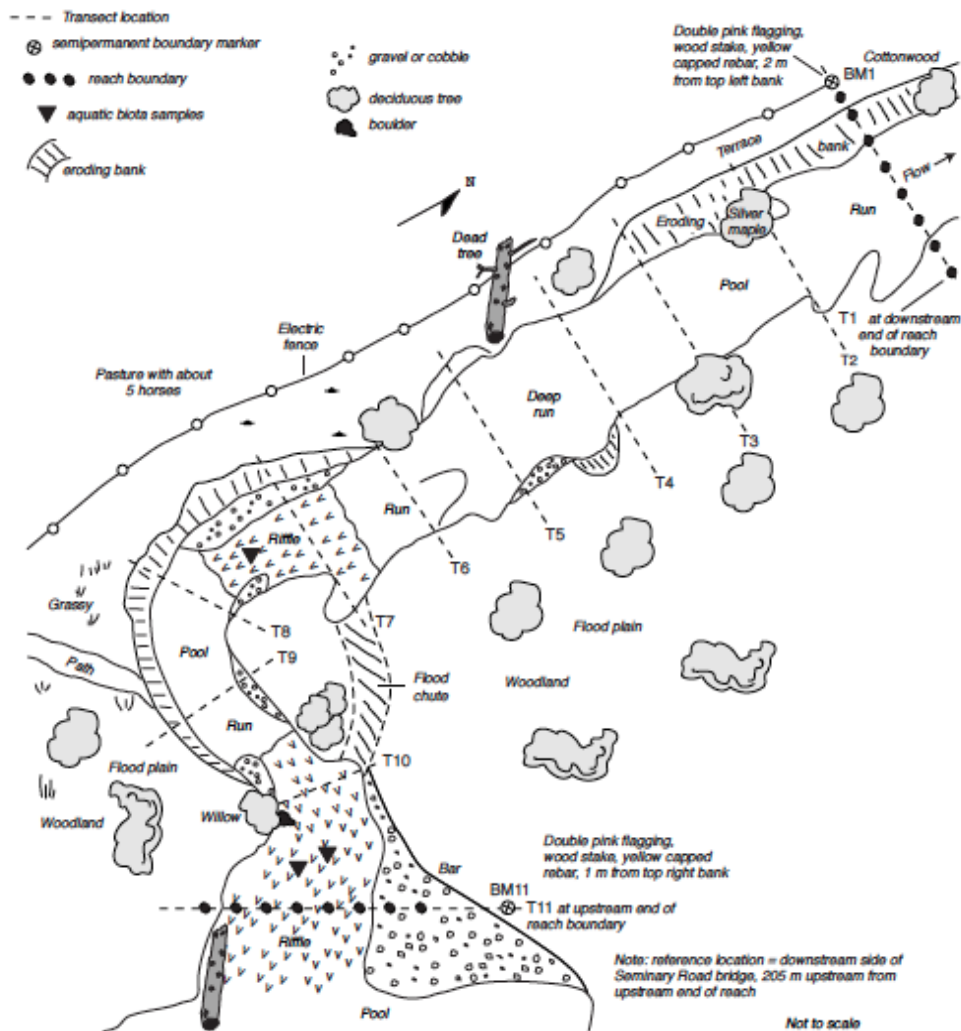


Figure 1.1: Example of the USGS-NAWQA survey method for a wadeable stream*

Generally, each transect is considered topographically accurate, but these data collection methods do not result in a spatially continuous datasets with high resolutions. Also, the established transect locations must be maintained for repeat surveys several months or years after they are created (Bangen et al., 2014a; Carbonneau et al., 2012; Fitzpatrick et al., 1998; Fonstad et al., 2012).

* Fitzpatrick, F.A., Waite, I.R., D'Arconte, P.J., Meador, M.R., Maupin, M.A., and Gurtz, M.E., 1998, Revised methods for characterizing stream habitat in the national water-quality assessment program, Water-Resources Investigations Report 98-4052: U.S. Geological Survey, Raleigh, NC, p. 24

1.1.2 Laser Scanning

Laser scanning (LS) is an active form of remote sensing that involves an airborne or ground-based laser emitting a pulse of electromagnetic radiation. The radiation gets reflected from ground surfaces and is then able to be detected so that the time of travel can be converted to distance of travel. Along with knowing the position of the laser, this information can be used to generate three-dimensional (3D) coordinates for the production of digital elevation models (DEMs) (Baltsavias, E.P., 1999; Lane and Carbonneau, 2007; Wehr and Lohr, 1999). Both airborne laser scanners (ALS) and terrestrial laser scanners (TLS) can produce accurate, high resolution DEMs. Laser scanners most commonly use near-infrared light, which does not penetrate water deeply, making it difficult to gather reliable submerged topographic data. At a much higher cost, blue-green laser scanners are available for bathymetric mapping. However, due to limited access to sensors, research using blue-green TLSs is still ongoing, particularly for shallower steams where the most common source of error is that the oblique scan angle increases the effects of refraction. Bathymetric Light Detection and Ranging (LiDAR) has typical mean errors of 0.10-0.30m with a typical spatial resolution of 1.00m. (Bailly et al. 2010; Bailly et al., 2012; Kinzel et al., 2013; Woodget et al., 2014).

Whether blue-green or near-infrared scanners are used, both TLS and ALS have been repeatedly shown to produce centimeter or millimeter (TLS) resolution topographic data, but these methods may not always be an option. For larger study areas (kilometers) , ALS may be worth the cost, while TLS is more likely to be preferred in smaller study areas (10s to 100s of meters) because the high cost of renting an ALS system would not be necessary and managing the equipment over larger areas is extremely time consuming and labor intensive. Both approaches require significant planning and post-processing. Furthermore, if characterizing

stream channel morphology change over time is the goal, repeat surveys would be necessary, drastically increasing the cost. Some local and state governments provide free access to ALS-derived data (largely near-infrared), but repeat surveys are not always available at convenient temporal resolutions (Bailly et al., 2012; James and Robson, 2012; Javernick et al., 2014; Lejot et al., 2007; Mertes, 2002; Woodget et al., 2014).

1.1.3 Digital Photogrammetry

Image matching methods have been around for more than 50 years, but not until the past two decades have these methods been widely used and accepted in fluvial geomorphology (Gruen, 2012; Lane et al., 2000). In traditional stereoscopic photogrammetry, image matching is done based on stereo-pairs in which software often requires nearly parallel images and ~60% overlap (James and Robson, 2012). Not only are stereo-pairs necessary to produce 3-D topographic data, but control points with known coordinates must also be visible in the images so that collinearity equations can relate the coordinates of the camera to the 3-D scene coordinates (James and Robson, 2012; Marcus et al., 2007; Woodget et al., 2014). In many geomorphological studies, digital stereo photogrammetry has become a popular alternative to ground survey and LS methods (Brasington et al., 2000; Lane et al., 2000, Woodget et al., 2014). Many photogrammetry-based studies have relied on stereoscopic aerial photographic pairs, but this methodology has not always been practical for smaller study areas because of the high cost of flights with high resolution calibrated cameras (Bertin et al., 2014; Gruen, 2012; Ouédraogo et al., 2014). Aerial photogrammetry has been shown to produce DEMs with 0.05-0.17m mean errors and 0.05-1.00m mean resolutions. With the increasing accessibility to suitable consumer-grade digital cameras, oblique and close-range photogrammetry have more recently been shown to produce sub-cm resolutions for what are typically smaller study areas (Bertin et al., 2015;

James and Robson, 2012; Lane et al. 2010; Westoby et al., 2012; Woodget et al., 2014). Close-range photogrammetry is much cheaper than aerial photogrammetry but requires more research in determining accurate submerged topography through the use of refraction corrections (Lane et al., 2010; Marcus et al., 2012; Woodget et al., 2014).

1.1.4 UAS and SfM-photogrammetry

Affordable UAS are one of the most recent advancements in traditional photogrammetry, but more recently UAS surveying has been coupled with structure-from-motion (SfM) photogrammetry (Clapuyt et al. 2012; James and Robson, 2012; Lejot et al., 2007). Much like traditional photogrammetry, the development of SfM photogrammetry began many decades ago, but the method hasn't been widely applied in geosciences until recently (Dietrich, 2015). Both methods rely on the input of images collected at multiple viewpoints in order to resolve the 3-D geometry of an object or surface (Fonstad et al., 2012). However, as opposed to traditional stereo pair-based photogrammetry, SfM uses more robust point matching algorithms to stitch together offset images that typically need much less overlap (Dietrich, 2015; Snavely et al., 2007; Westoby et al., 2012). This drastically increases the ease of use for SfM when compared to traditional photogrammetry because the SfM algorithms automatically solve for not only the geometry of the scene, but also the cameras' orientations and relative positions. Other photogrammetric methods typically require more manual input of GPS data and camera calibrations, typically relying on camera-mounted GPS or post-hoc triangulation (Dietrich, 2015; Snavely et al., 2007; Westoby et al., 2012). Thus, SfM software can account for camera calibration to resolve 3-D structure by gathering camera settings such as focal length information from exchangeable image file format (EXIF) tag standards (Snavely et al., 2007). Camera orientations and positions are determined simultaneously with the identification of matching

features amongst images. This process results in the production of a point-cloud that can be used to generate a 3-D mesh, but without defining a coordinate system, these structures only exist only in an "image-space" coordinate system with no reference to the real world. However, the process of manually selecting a few corresponding points across images, with known real world coordinates, has been made relatively simple by commercially available SfM software. This selection process can be made easier by placing high contrast physical targets in the study area prior to image acquisition (Clapuyt et al., 2015; Dietrich, 2015; Fonstad et al., 2012; Javernick et al., 2014; Snavely, 2007; Westoby et al., 201).

Alongside SfM reliably automating image-based surface restitution, the increasing ease and affordability to acquire high resolution imagery has also made photogrammetry-based studies more common in the field of geomorphology, but over the past several years, UAS have also provided significant improvements in image acquisition (Fonstad et al. 2015; Westoby et al., 2012). Both fixed and rotary-winged UAS have become more affordable, lightweight, and better suited for image acquisition (Woodget et al., 2014). Photogrammetry-based topography traditionally relied on satellite imagery and manned aerial system (MAS), but these methods are typically lower resolution and/or expensive. The emergence of small, affordable UAS has made topographic remote sensing has shown promise in increasing spatial and temporal resolutions (Turner et al., 2013; Woodget et al., 2014). The ability of small UAS to fly at lower altitudes allows for the increase in spatial resolution (on the order of 1cm/pixel), and the ease/cost of use makes repeat surveys more reasonable (Turner et al. 2013). Furthermore, in the case of fluvial remote sensing, SfM has been coupled with MAS-based imagery for larger study areas, but the availability of UAS makes it more cost effective to survey both larger and smaller study areas

(Clapuyt et al., 2015; Dietrich, 2015; Lejot et al., 2007; Turner et al; 2015; Westoby et al., 2012; Woodget et al., 2014).

1.2 Study Overview

This study focused on topographic data collection at multiple sites in the Atlanta, GA area to compare UAS-based SfM photogrammetry to traditional stream survey methods, particularly the USGS-NAWQA method. In total, three areas were surveyed using these methods. The first location was on Proctor Creek, northwest of Atlanta. The work at this site was done as part of a group effort for a seminar class in geomorphology and hydrology. The purpose of the collaborative group project was to make an attempt at using SfM-based photogrammetry, because this was a remote sensing method unfamiliar to the class, which was comprised of Georgia State University (GSU) graduate students. The project resulted in a partial and discontinuous SfM-derived DEM. Although the results were incomplete, the project showed promise for continued work.

The Proctor Creek study resulted in an incomplete DEM, because there was not enough imagery coverage for the SfM software to resolve the entire study area. However, the project made it possible for the group members to become more familiar with operating a drone and using SfM software. Thus, this study was made possible through these initial efforts, and two additional study areas were added to test SfM photogrammetry as a method that could be used in fluvial geomorphology.

In order to minimize difficulties in imagery coverage, the first study area added was selected based on its relatively low vegetation. This location was along the narrow and shallow South Fork Peavine Creek (SFPC) within the Druid Hills Golf Course (DHGC). After the work done at this site was successful in generating a continuous DEM with a relatively high resolution,

another site was chosen along North Fork Peachtree Creek (NFPC). This site was chosen because of its similarity with the Proctor Creek study area, in that it posed more difficulty with depth, total coverage, and vegetation relative to the SFPC location.

Once DEMs were created, it was then possible to extract transects from the DEMs that were spatially congruent with the total station transects. The total station transects and other surveyed points were then compared to DEM transects. For the Proctor Creek study area, the transects were only compared visually, but for SFPC and NFPC, the bankfull width (BW) and bankfull depth (BD) were determined from the transects to be compared to one another. Total station points surveyed outside of the transects were compared to z-values of the DEMs.

1.2.1 Site Locations

The first study area occurs along Proctor Creek in Fulton County, northwest of downtown Atlanta (Fig. 1.2). The property is privately owned as the Pet Heaven pet cemetery, and there is a USGS stage monitor at the bridge to the east of the study area.

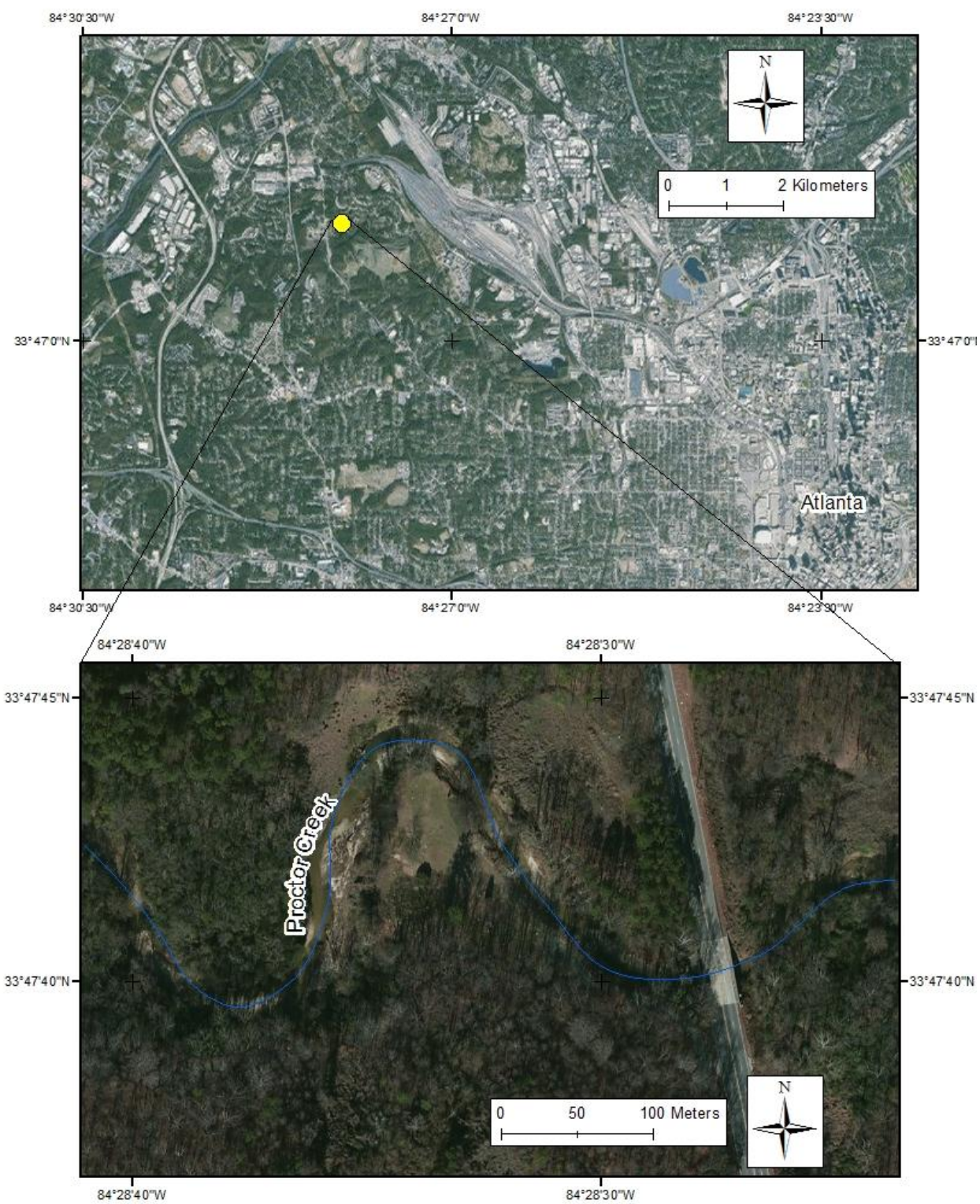


Figure 1.2: Study area on Proctor Creek in Fulton County

The second study area occurs along South Fork Peavine Creek in DeKalb County, Georgia within the Druid Hills Golf Course (Fig.1.3).

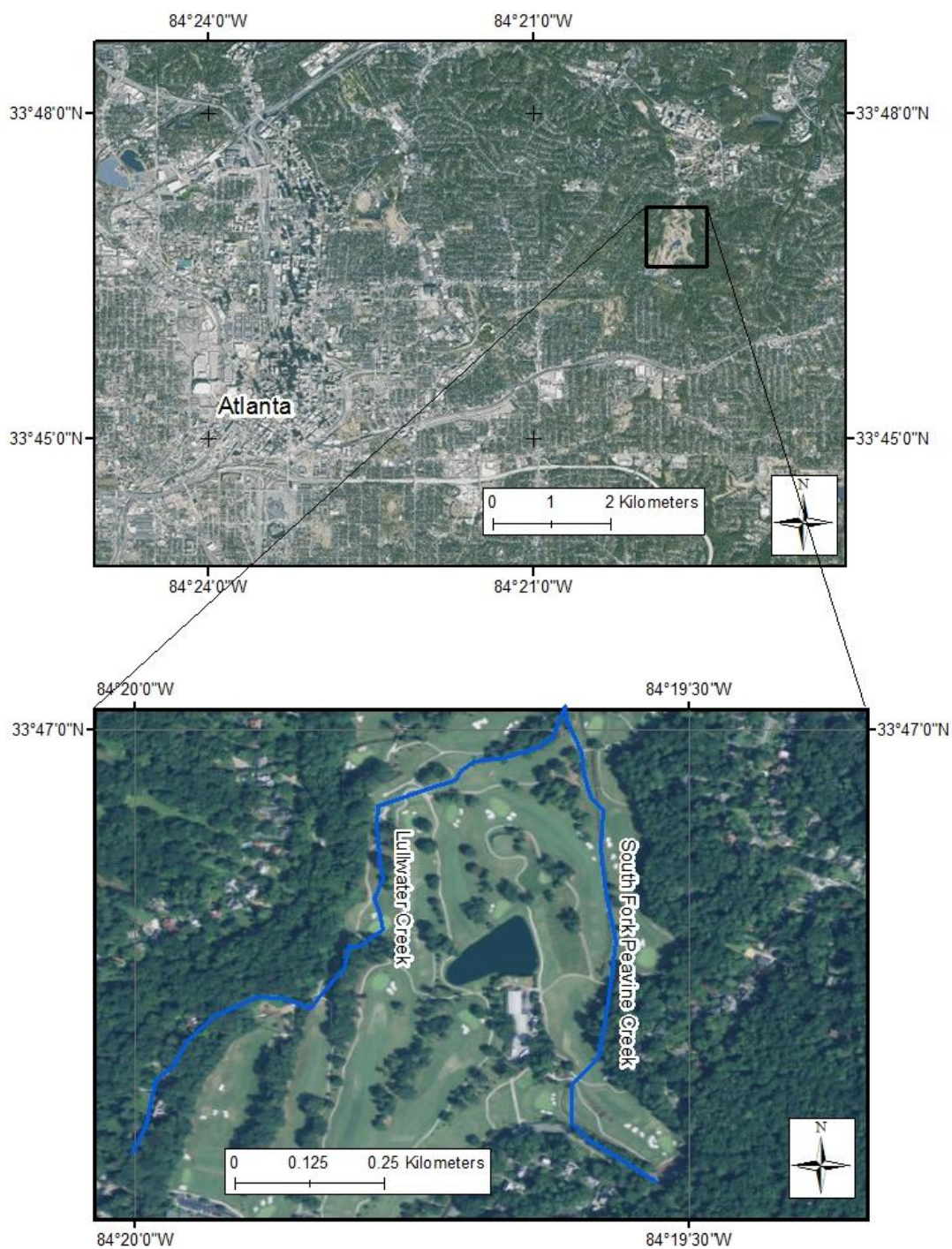


Figure 1.3: Study area on South Fork Peavine Creek in DeKalb County, Georgia

The third study area occurs along North Fork Peachtree Creek in DeKalb County, between Buford Highway and I-85 (Fig. 1.4).

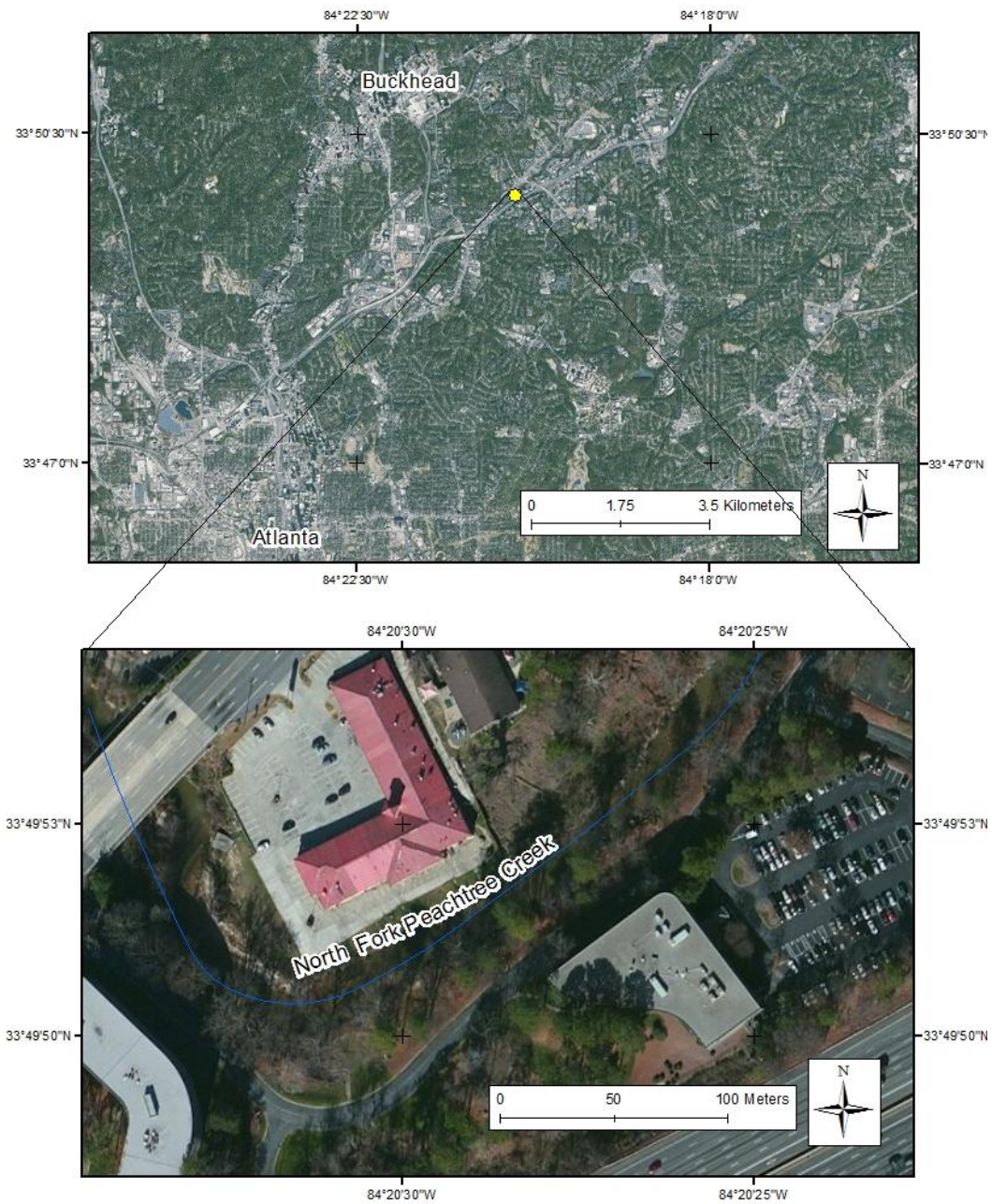


Figure 1.4: Study area on NFPC in DeKalb County, Georgia

1.2.2 Study Purpose and Significance

The purpose of this study is to evaluate the accuracy of SfM-derived fluvial topographic data in comparison to transects surveyed according to the USGS-NAWQA method. In addition to accuracy, ease of use will also be considered, as this is considered one of the major benefits of UAVs coupled with SfM. Within the past couple of decades, high resolution surveying has become increasingly applied in fluvial geomorphology, particularly in the form of laser scanning technologies and traditional photogrammetry. These methods have been used as an alternative to total station surveying because it is viewed as time consuming, labor intensive, and it results in coarsely spaced, spatially discontinuous transects, which require increased interpolation. Although total station surveying has been a widely used method, repeat surveys and the number of total surveyed stream segments are limited, which inhibits tracking morphological change over time. Similarly, laser scanners and the aerial vehicles used in surveying are costly, also making repeat surveys difficult.

Perhaps the most recent and emerging technology in fluvial geomorphology surveying is SfM photogrammetry coupled with UASs. Just within the past few years, this application has been showing up in academic literature, and because it is not an accepted method, studies still focus on comparing SfM photogrammetry to widely used methods such as laser scanning and total station surveying. However, when SfM is compared to total station surveying, scattered control points, rather than equally spaced transects, are often compared to the total station points. Regardless of which methods are compared, most studies share one idea in common, and that is to suggest that SfM coupled with UASs holds promise as a relatively cheap and therefore repeatable method of producing high resolution (cm to mm) topographic data of fluvial landforms.

The goal of this study is to provide further testing of this new method, but it may be unique in that it compares SfM derived DEMs to transects collected according to the USGS-NAWQA method. This traditional method of tracking geomorphological change is accepted as accurate and has been used in reporting on changes in fluvial geomorphology. It is not as expensive as laser scanning, but it requires many hours of field work. This study will focus on comparing the two methods to try to determine if SfM coupled with UASs shows promise as an alternative method, possibly preferred for its low cost, ease of repeat surveys, and delivery of high resolution topographic data.

2 Methods

This study required the generation of total station transects collected at each site location alongside imagery of the area. Total station data and imagery were collected on the same day to ensure little or no disparities in water level or geomorphology between the two datasets. Total station data was spatially referenced to be used in a GIS, while the imagery was processed using Agisoft's Photoscan Pro (versions 1.1.1 through 1.2.4). Once the DEM was generated, transects corresponding to the total station transects were extracted from the DEM to be compared for accuracy.

2.1 Total Station Transects

The total station transects were collected according to the USGS-NAWQA method. However, at the NFPC study area, the segment length was shortened due to access limitations. The USGS-NAWQA method required a stream segment length of 150-200 meters, but only 100 meters were surveyed, with 11 equally spaced transects occurring every 10m, starting at the 0m mark.

2.2 Control Points

Although it is not necessary in order to create a SfM-derived DEM, ground control points (GCPs) were placed along the banks of and in the bed of each stream so that they could be surveyed and visible in the imagery. These points are meant to be easily identifiable in photos, thus brightly painted Styrofoam balls and bricks were used (Fig 2.1). The ease of identification makes it easier for Photoscan and the user to select these points in each image. Once identified in Photoscan, the points are used to aid model construction by speeding up image matching using

these predetermined matching. Furthermore, the points can then be used to compare across both methods using their DEM and total station z-values.



Figure 2.1: Image taken during flight at the DHGC site location showing the GCPs placed along the reach banks and in the stream bed

At least 20 painted GCPs were used at each site, and the location of each GCP was measured using the total station. Also, for every submerged GCP, the depth of the object was also recorded. The 3-D coordinates for each point were used to orient the SfM model in real space.

2.3 Image Acquisition

The photos were taken with a 10 MP GoPro camera attached to a DJI Phantom II quadcopter. The Phantom II weighs approximately 1kg and has a range of 1km (in an open area), and each LiPo battery allows for about 25 minutes of flight time (Fig 2.2).



Figure 2.2: DJI Phantom II with a 10 MP GoPro camera attached to a Zenmuse 3-axis gimbal*

The camera is mounted to the quadcopter via a Zenmuse 3-axis gimbal, which stabilizes the camera during flight. The rotation of the gimbal can also be changed using the Phantom remote controller, allowing 45° of rotational movement. Images that were used for SfM modeling were taken facing directly down, rather than forward facing or oblique, because it was assumed that this may help reduce distortion.

2.4 Image Selection

After image acquisition, photos were manually selected based on apparent adjacency, quality, and coverage. This process is largely subjective, but initially blurry images were removed, as well as those outside of the study area or with no adjacency to it. In general, the goal for selecting images for SfM is to reduce redundancies and take photos from as many different viewpoints as possible, while still maintaining a sufficient amount of overlap. For this reason, some images that were taken from viewpoints that were very close to one another, were removed. Image selection is a relatively quick process but is valuable because it can vastly

* <http://store.dji.com/product/phantom-2>

reduce the number of photos, which lowers processing time significantly. However, if the model is generated and there appears to be image coverage lacking in some areas, images can be added back into the model to help correct any problem areas.

2.5 SfM Processing

Photos were processed using Agisoft's PhotoScan Pro (version 1.1.6), a commercially available SfM software package (Agisoft LLC, 2013). Other, free SfM packages are available, but PhotoScan Pro was made available through the Collaborative University Research & Visualization Environment (CURVE) at Georgia State University. Furthermore, PhotoScan Pro has been shown to be successful in similar studies, and it contains the routines necessary to output georeferenced DEMs (Woodget et al., 2014; Javernick et al., 2014). After image selection, the workflow in PhotoScan is comprised of these 8 steps: 1) import images, 2) align images, 3) identify GCPs, 4) georeference, 5) re-align, 6) generate dense cloud, 7) build geometry ("mesh"), and 8) build texture. Aligning the photos, generating the dense cloud, and building the mesh are all processes that can take PhotoScan several minutes to several hours (possibly days) to complete, depending on the number of images, the resolution of the images, the chosen processing parameters, and the processing speed of the computer.

Once the images are imported, they must first be aligned, a process which finds common points amongst the photos and generates a sparse point cloud. This step also determines the position of the camera for each image and refines the camera calibration parameters based on the EXIF tags. Once the photos are aligned, the GCPs must be identified within each of the photos they are captured in. This process is done both manually and automatically because, after GCPs are manually identified in a few photos, PhotoScan begins estimating the positions of those points in all other images they are in. The estimations made by PhotoScan can then be quickly

confirmed or rejected by the user. Typically, the higher the contrast of the GCPs, the better PhotoScan will be at estimating their locations.

After the GCPs are identified, their XYZ coordinates (northing, easting, and elevation) can be entered into PhotoScan. Then the photos must be re-aligned with this new data, but the introduction of control markers typically decreases processing time. Once re-aligned, the dense cloud can be generated. If desired, PhotoScan can then be used to generate the 3-D model with texture, and the model can be exported as a raster file. However, it is also possible to export the dense cloud in .las format and treat the data as though it were LiDAR. For this study, the georeferenced dense cloud was used to ultimately generate DEMs. Before the DEMs are created, the dense point clouds serve as the first visual aid in the SfM process to see how well the model is being constructed. Areas that did not receive adequate coverage are left blank, and areas where vegetation disrupted the scene are often rough due to blocked views of the river landscape (Fig. 2.3 and 2.4).



Figure 2.3: Images of the SFPC dense point cloud

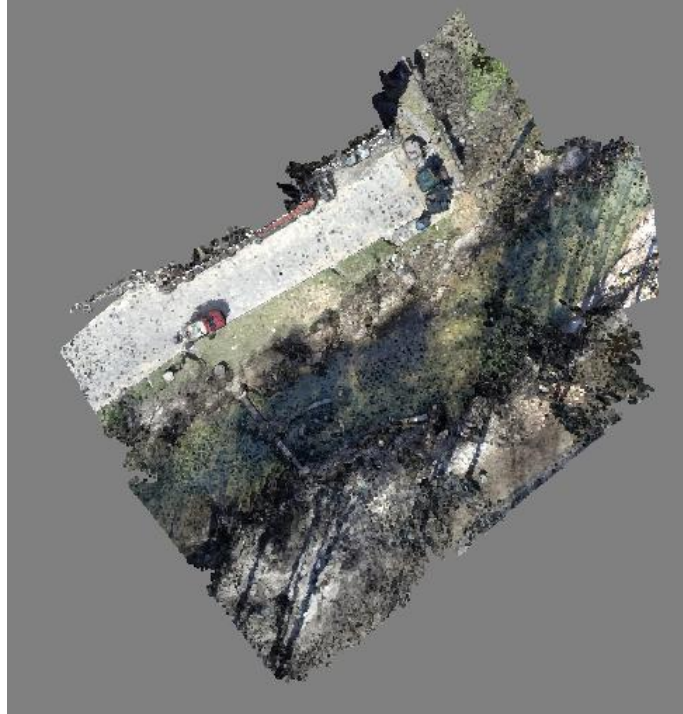


Figure 2.4: Images of the NFPC dense point cloud

2.6 Quantitative Topographic Data Comparison

Topographic data from the total station and the DEM were compared using descriptive statistics within Microsoft Excel. For both SFPC and NFPC, the BW and BD values were determined for both transect sets, and the percent differences were determined between the two, working under the assumption that the total station values are the "known" or reference values. Control points were also compared for both sites to determine how well the DEM estimated the z-values of the random points that occurred outside of the transects. These were compared by being plotted against one another so that a simple linear regression could be made with p and r^2 values.

3 RESULTS

3.1 SfM Processing

For each site, the DEM generation process requires a generation of a 3D model, and it also requires the input of GCP spatial reference information. Possibly due to coverage issues, not every GCP was resolved completely by Photoscan. Thus, each site began with more GCPs than were used for processing. For each site, models and example imagery are provided, as well as flight information to show how flight decisions may affect coverage.

3.1.1 *Proctor Creek*

Because of the reach size at the Proctor Creek study area, imagery and transects were collected on two separate days. This also required imagery to be separated into 3 separate sections, defined as "chunks" by Agisoft's Photoscan. This was done to reduce the amount of processing time required so that the 3 chunks could be merged together after each one was completed individually.

The upstream chunk (Fig. 3.1) of the stream segment resulted in the most complete DEM and required a total of 206 photos to generate the model. There were 5 ground control points used for spatial reference. The middle chunk used 87 images, and the downstream chunk used 71 images. Tall trees can be seen (Fig. 3.2) in the study area, which often required a high flying altitude, compromising resolution. This also made it so that GCPs were not always visible even though they existed in the scene.

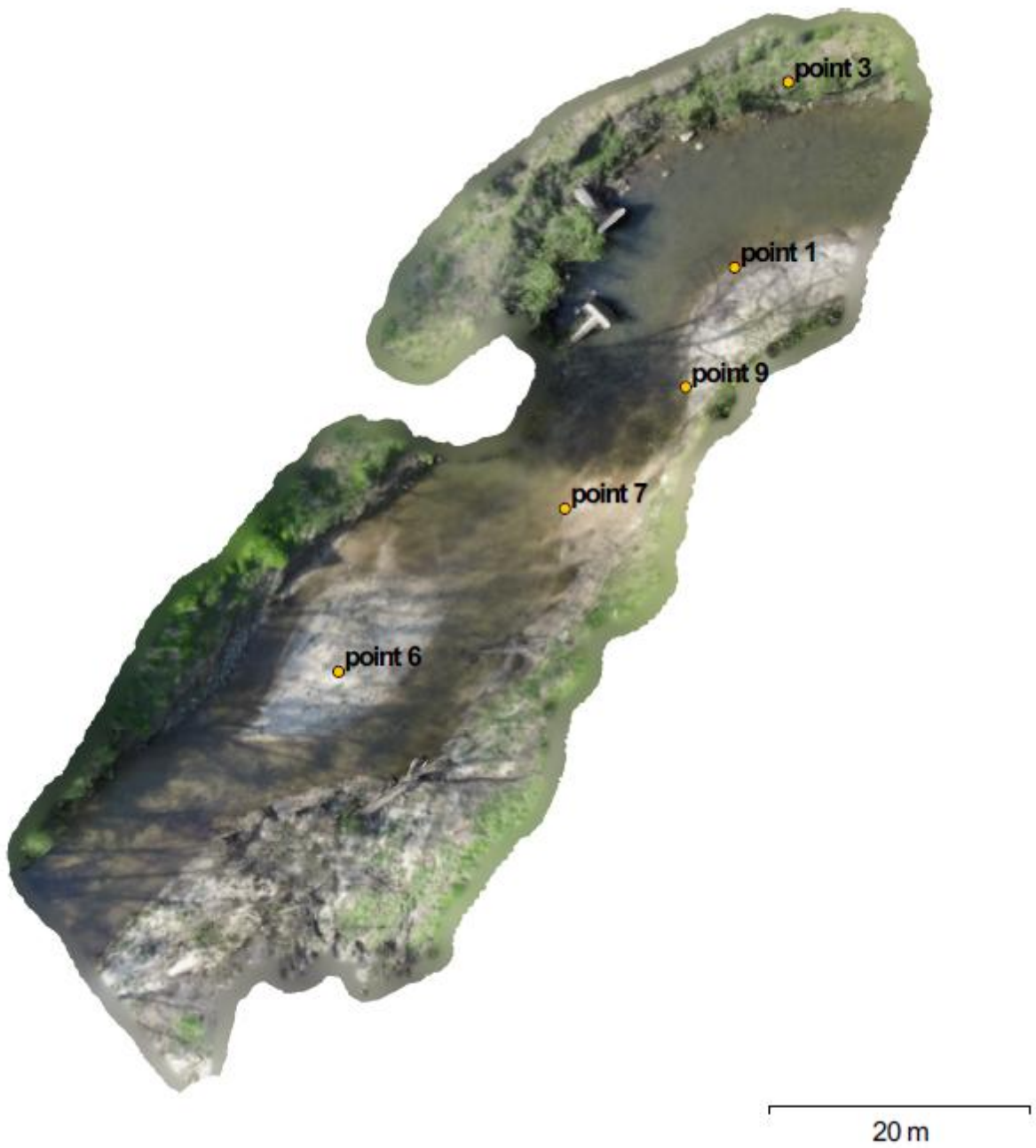


Figure 3.1: SfM model of the upstream chunk at Proctor Creek also showing GCPs



Figure 3.2: Examples of drone-based aerial imagery of the Proctor Creek study area

Because of the tall trees, the average flying altitude was 26.15m for the upstream chunk, which resulted in good image overlap. However, the imagery locations reveal a sporadic pattern that likely varied significantly in altitude (Fig. 3.3).

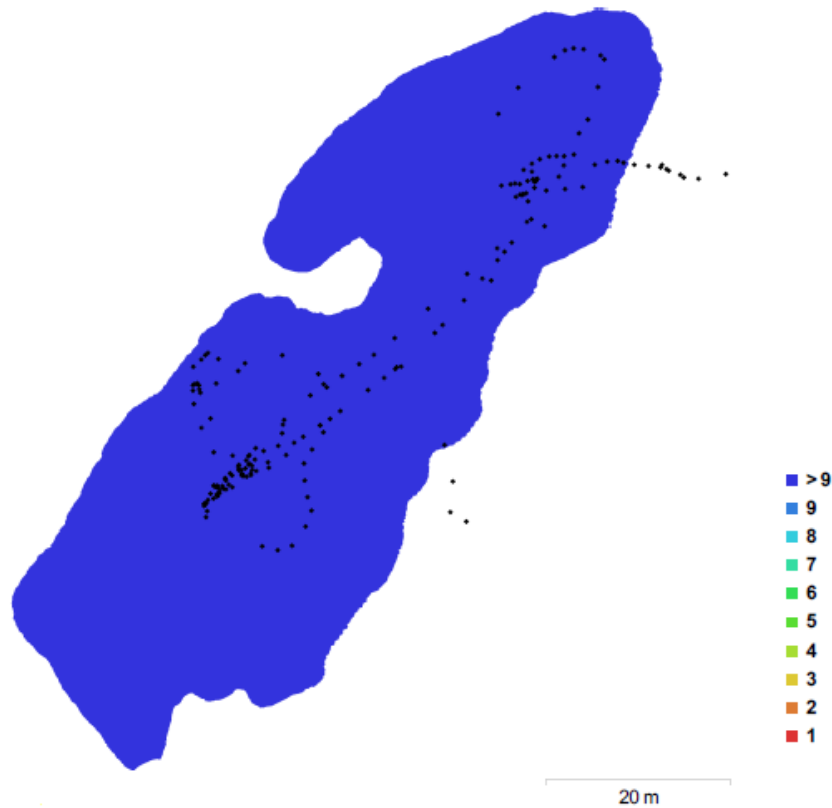


Figure 3.3: Locations where images were taken shown with image overlap statistics for the upstream chunk at Proctor Creek

3.1.2 South Fork Peavine Creek

The DEM and 3D model created for SFPC at DHGC used 507 images and 5 georeferenced control points (Fig. 3.4). More than 20 GCPs were originally placed and surveyed in the scene, but not all points were aligned and projected properly into the model and could not be used for spatial reference. Similarly, more than 1300 images were originally taken of the

scene, but only those with top-down views and appropriate adjacencies were eventually used (Fig 3.5).



Figure 3.4: SfM model of the SFPC stream segment showing the locations of GCPs used as spatial reference



Figure 3.5: Example of drone-based imagery of SFPC. The top photo was not ultimately used in the generation of the model and DEM

Although multiple attempts were made at generating a 3D model and DEM, the final DEM used in this study took over 40 hours of processing time to complete, with the alignment taking the most time at nearly 19 hours. However, this total processing time is likely less than was spent on all three chunks for the Proctor Creek Project, and more photos were used for

SFPC. Furthermore, the average flying height was much lower at 7.41m, as there was less focus on large extent imagery and more focus on tightly spaced, low altitude imagery (Fig 3.6).

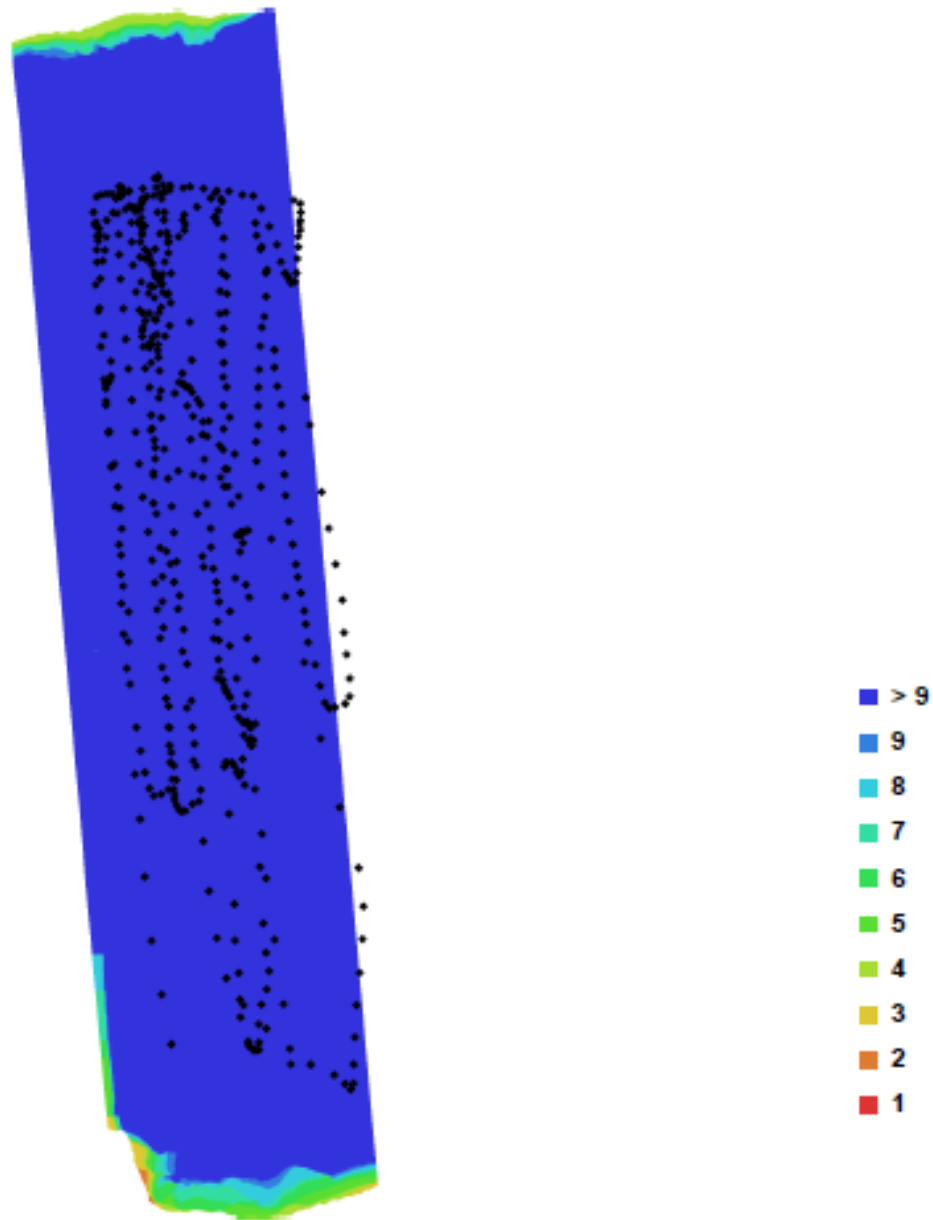


Figure 3.6: Locations where images were taken shown with image overlap statistics for SFPC

3.1.3 North Fork Peachtree Creek

The DEM and 3D model created for NFPC used 937 images and 14 georeferenced control points (Fig. 3.7). More than 20 GCPs were originally placed and surveyed in the scene, but not all points were aligned and projected properly into the model and could not be used for spatial reference. More than 1600 images were originally taken of the scene and due to the size of the stream segment, images were taken at drastically variable altitudes as an attempt to ensure adequate coverage (Fig 3.8).

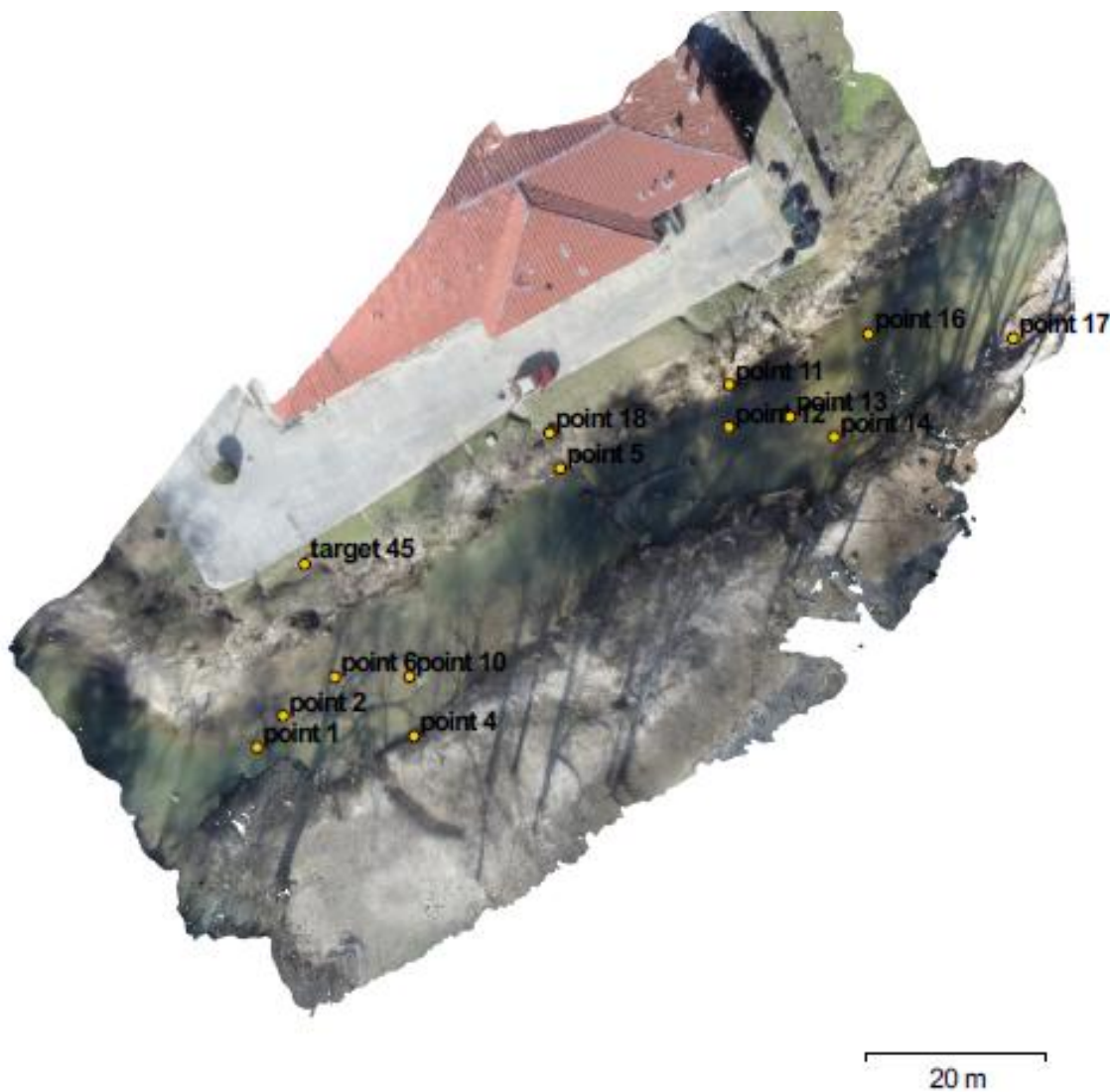


Figure 3.7: SfM model of the SFPC stream segment showing the locations of GCPs used as spatial reference



Figure 3.8: Example of drone-based imagery of NFPC. Both photos were used in model generation

The final DEM used in this study took over 70 hours of processing time to complete, with the alignment taking the most time at about 34 hours. With an average of 13.4m, the flying altitude for NFPC was higher and more variable than SFPC. Some images were taken closer to the water while some nearly captured the entire scene. This resulted in good image overlap, but the flight pattern does not appear as uniform as that of SFPC (Fig. 3.9).



Figure 3.9: Locations where images were taken shown with image overlap statistics for SFPC

3.2 Transects and DEMs

For each site, SfM-derived DEM transects and total station transects were generated. The DEM transects locations were chosen based on their best fit to the total station transect start and end points. This was done because human error always causes total station transects to be nonlinear as surveyors wander slightly from point to point, resulting in slightly irregular transects.

3.2.1 *Proctor Creek*

For the Proctor Creek study area, the imagery coverage was not sufficient enough to merge all 3 chunks together. Furthermore, most of the DEM transects were unable to match the lengths of the total station transects (Fig. 3.10). In an effort to initially fix some of these problems, multiple DEM attempts were made using various imagery inputs, but each attempt resulted in an incomplete stream segment DEM and insufficient DEM transect lengths (Fig. 3.11).

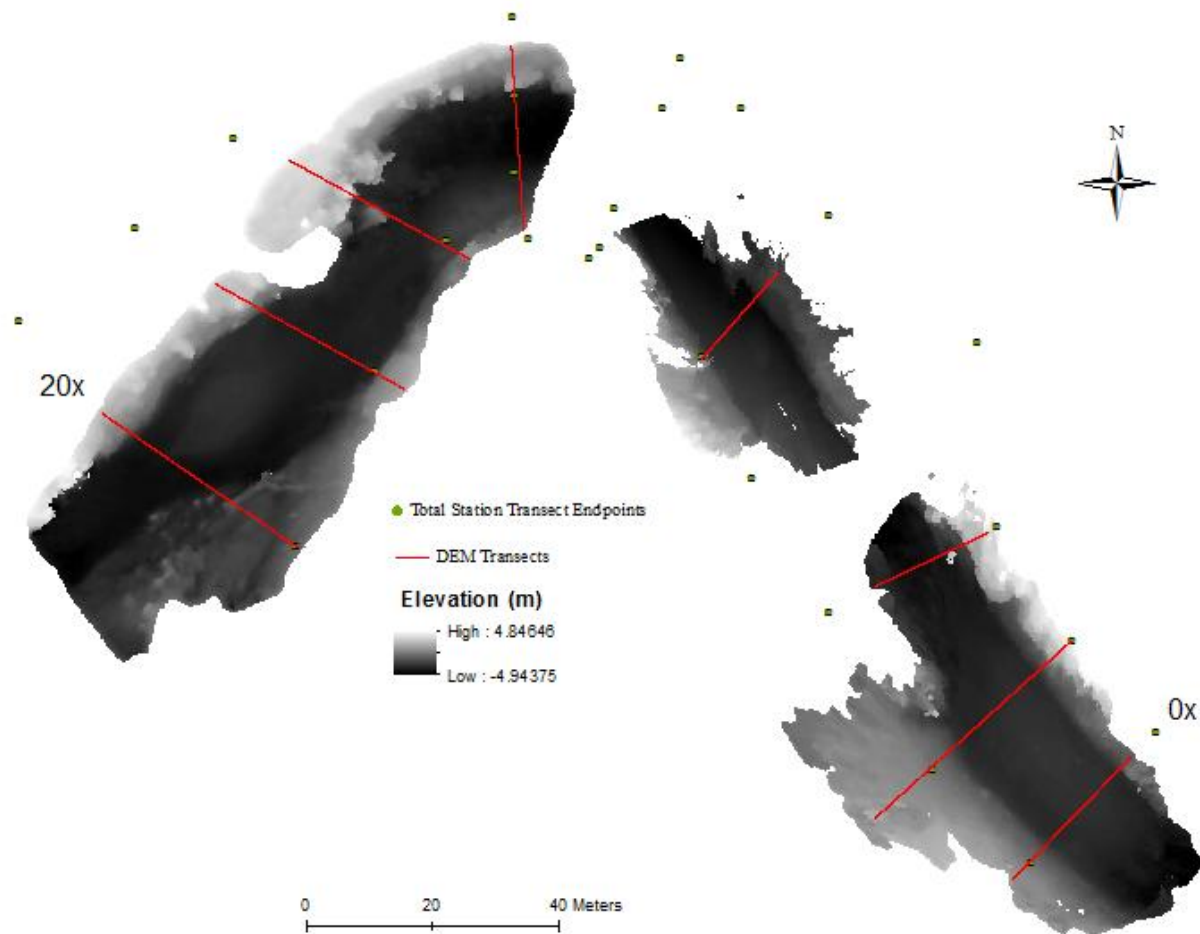


Figure 3.10: Proctor Creek at Pet Heaven. SfM-derived DEM shown with TS transect start and end points as well as DEM transect locations

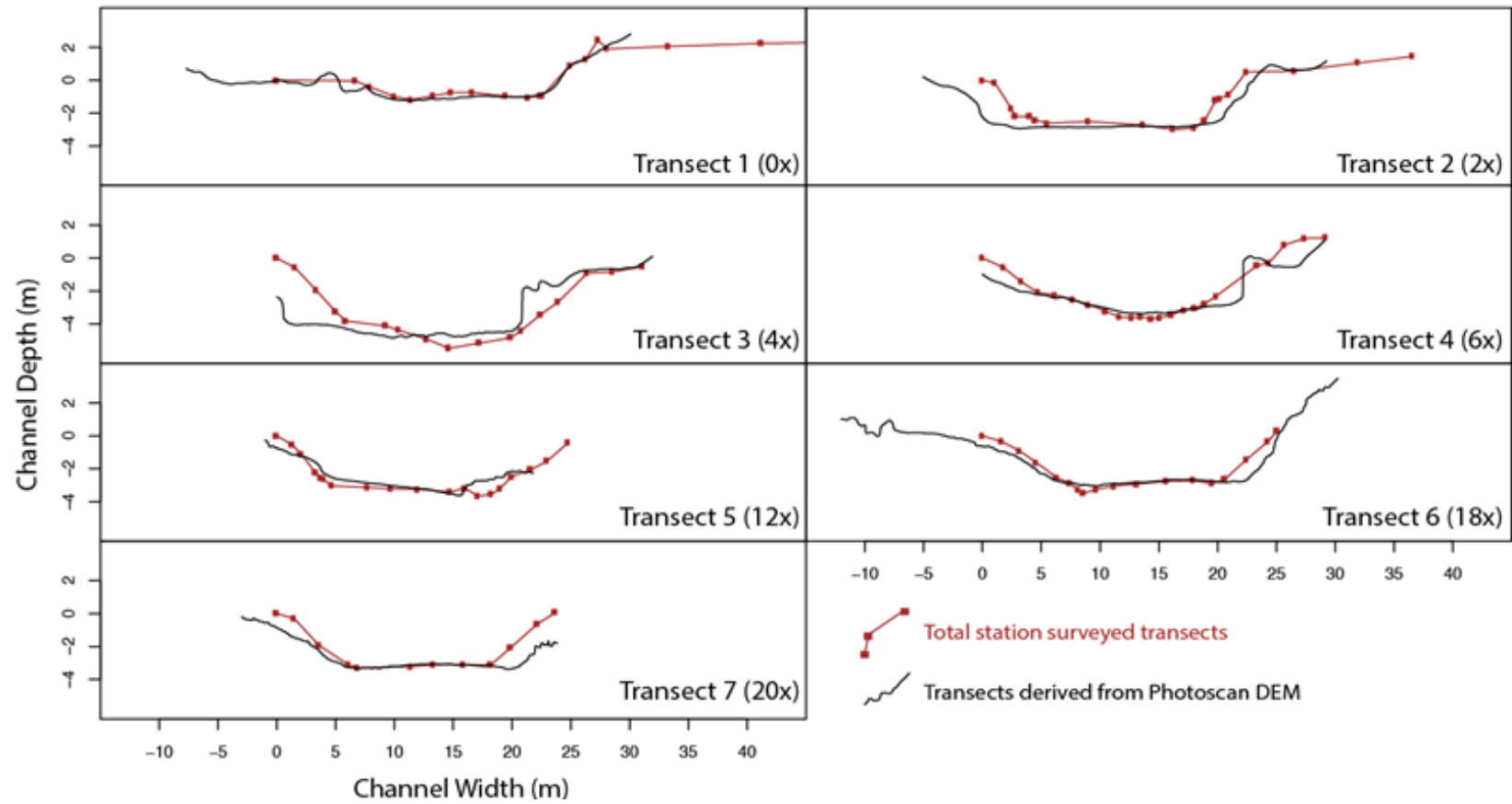


Figure 3.11: Proctor Creek DEM and TS transects plotted atop one another

Despite the lack of coverage, the DEM transects showed some promise for future study areas, as their morphologies closely resembled that of the TS transects.

3.2.2 *South Fork Peavine Creek*

The DEM created for SFPC has a resolution of 2.76cm (Fig. 3.12). The model was processed as one contiguous chunk with sufficient coverage for each DEM transect (Fig. 3.13).

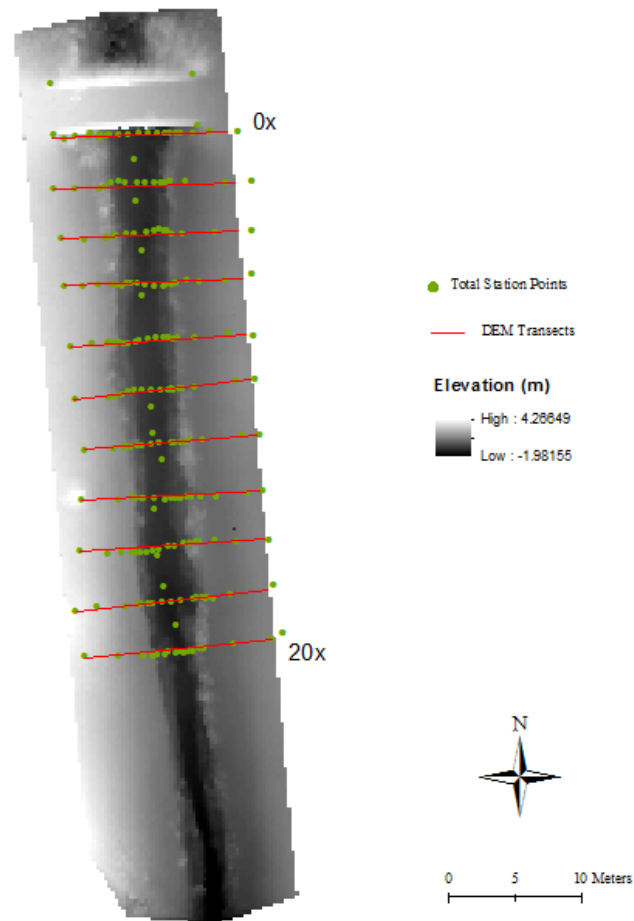


Figure 3.12: South Fork Peavine Creek at DHGC. SfM-derived DEM shown with TS points as well as DEM transect locations

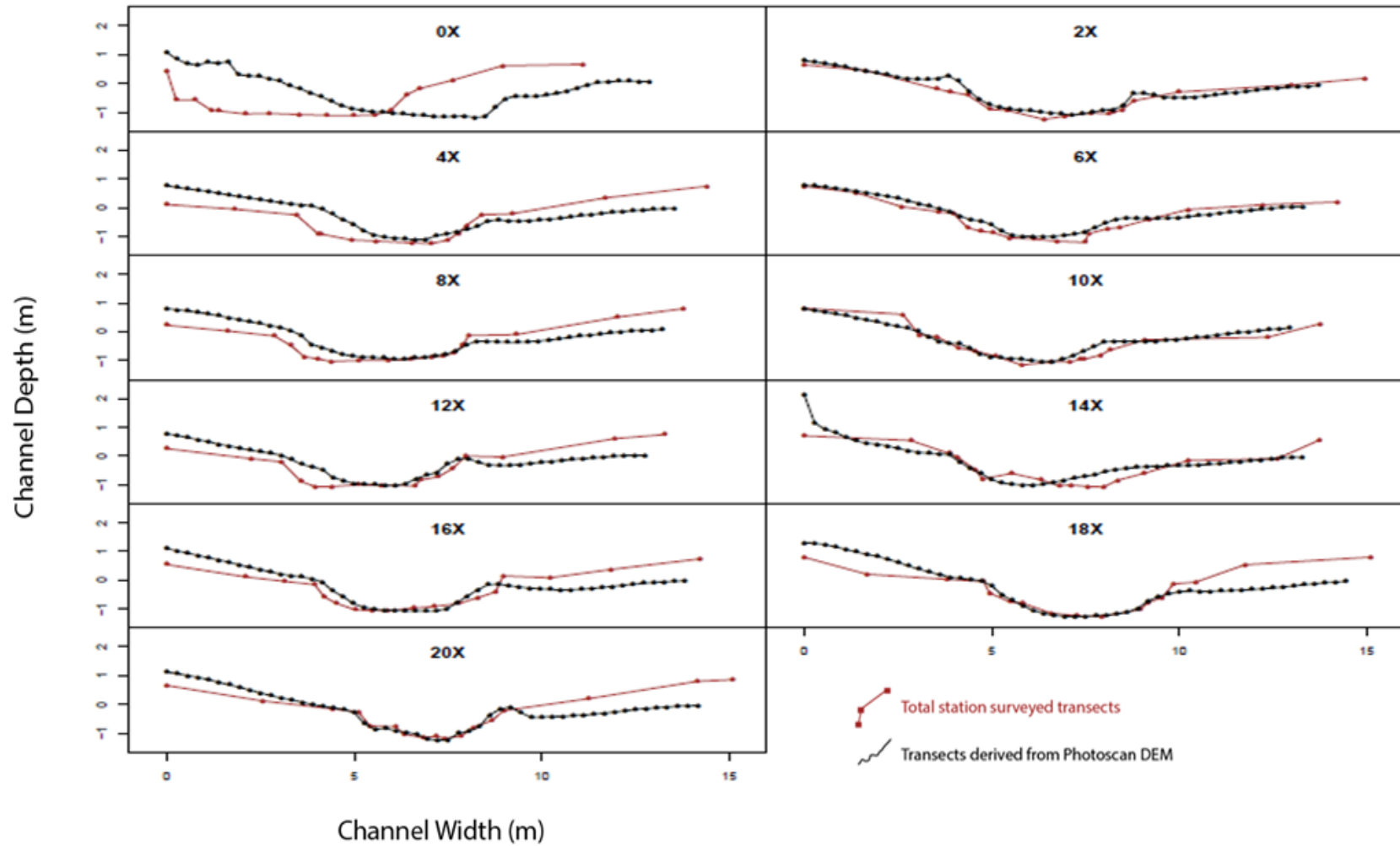


Figure 3.13: SFPC DEM and TS transects plotted atop one another

With the exception of 0x, the SFPC DEM transect profiles appear to closely resemble the TS transect profiles, perhaps even a better visual match than the Proctor Creek transects. However, at least 7 of the DEM transects clearly underestimate the land surface relative to the TS transects.

3.2.3 North Fork Peachtree Creek

The DEM created for NFPC has a resolution of 2.9cm (Fig. 3.14). The model was processed as one contiguous chunk with sufficient coverage for each DEM transect (Fig. 3.15). Unlike SFPC, the transect set includes 0x through 10x (where x is the channel width) with a 1x spacing.

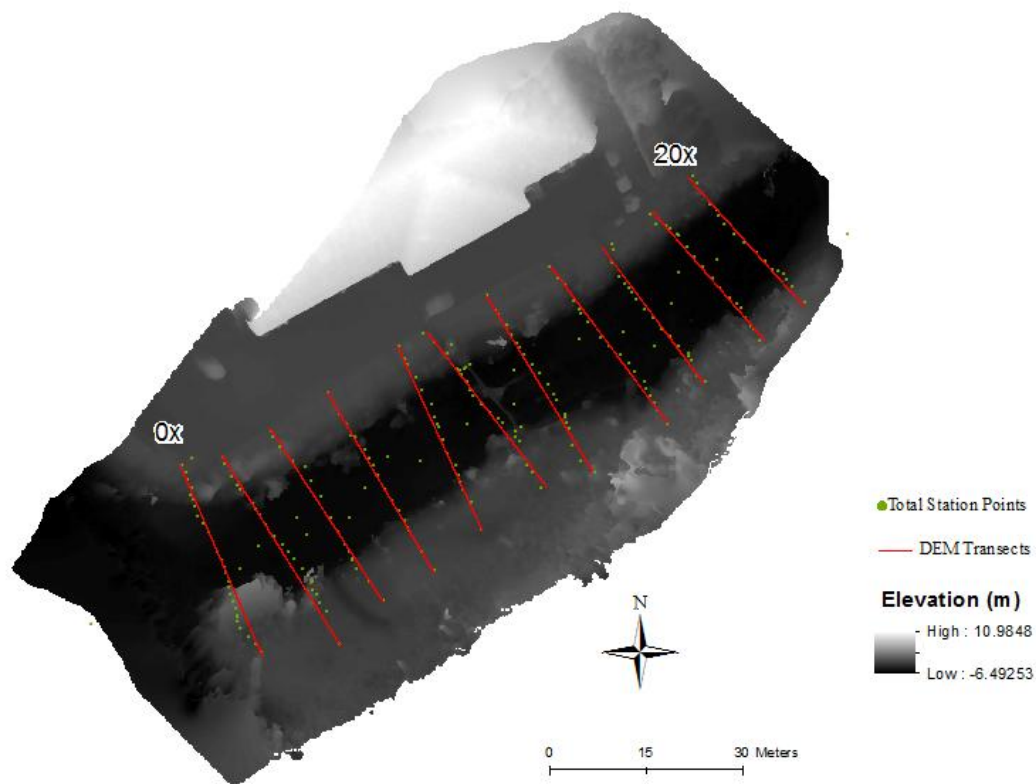


Figure 3.14: North Fork Peachtree Creek SfM-derived DEM shown with TS points as well as DEM transect locations

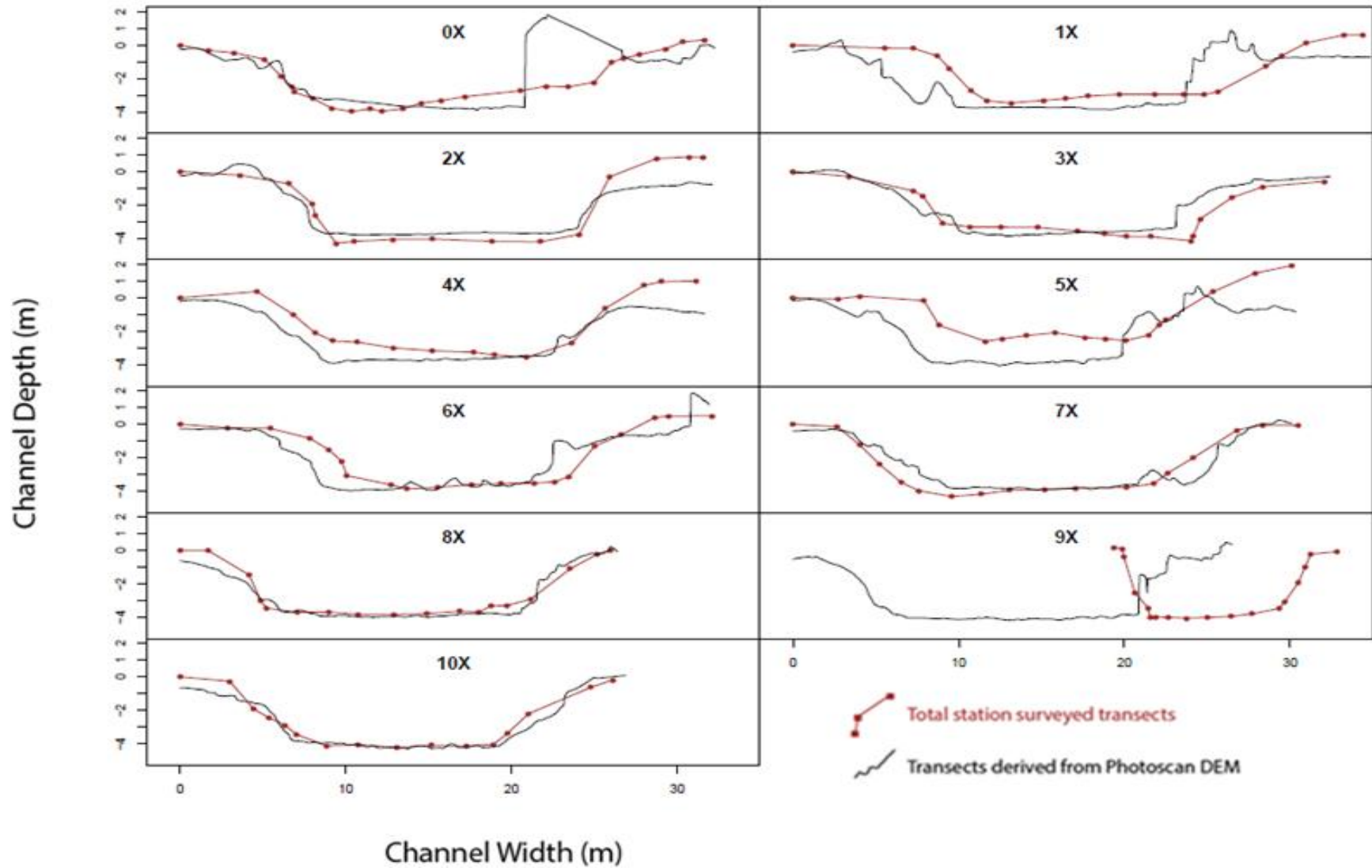


Figure 3.15: NFPC DEM and TS transects plotted atop one another

The transects that immediately appear to have the most issues matching well are 0x, 1x, 4x, 5x, and 9x. The area where the DEM transect rises above the TS transect for 0x was an area of thick vegetation that was difficult to get land surface imagery but also difficult to survey with the TS. What stands out about 1x, 4x, and 5x is the DEM often overestimates the stream bed and land surface. For 9x, the DEM transect appears successful, but unfortunately there was some unknown error with the TS transect, thus the two cannot be compared.

3.3 Quantitative Topographic Data Comparison

3.3.1 *South Fork Peavine Creek*

The percent differences between DEM and TS BW and BD values range from 1.0 to 48.7 and 1.1 to 53.3, respectively (Table 3-1). The linear regression for the TS and DEM control point z values show an R^2 value 0.31 where $n = 10$ (Fig. 3.16). The standard error and the p-value are, respectively, 0.051 and >0.05 . Without the outlier, the R^2 value, standard error, and p value are 0.33, 0.051, and >0.05 .

Table 3-1: TS and DEM BW and BD values for SFPC, as well as the percent difference between these values

Transect	Total Station (m)		SfM DEM (m)		Absolute Difference (m)		Percent Difference (%)	
	BW	BD	BW	BD	BW	BD	BW	BD
0x	5.5	0.55	5.2	0.74	0.31	0.19	5.8	29.5
2x	5.1	0.85	4.4	0.74	0.75	0.11	15.7	13.8
4x	4.9	1.00	3.9	0.65	1.04	0.35	23.5	42.4
6x	6.8	1.14	4.2	0.66	2.67	0.48	48.7	53.3
8x	5.2	0.89	4.6	0.63	0.58	0.26	11.9	34.2
10x	5.1	0.88	4.7	0.71	0.37	0.17	7.6	21.4
12x	4.5	0.86	4.7	0.95	0.16	0.09	3.5	9.9
14x	5.9	0.92	3.9	0.54	1.99	0.38	40.7	52.1
16x	5.0	0.90	4.4	0.91	0.59	0.01	12.7	1.1
18x	4.7	1.1	4.8	0.9	0.05	0.23	1.0	23.4
20x	3.5	0.91	3.6	0.96	0.12	0.05	3.4	5.3
Mean					0.8	0.2	15.9	26.0
Median					0.6	0.2	11.9	23.4
Std. Dev.					0.8	0.1	15.7	18.0

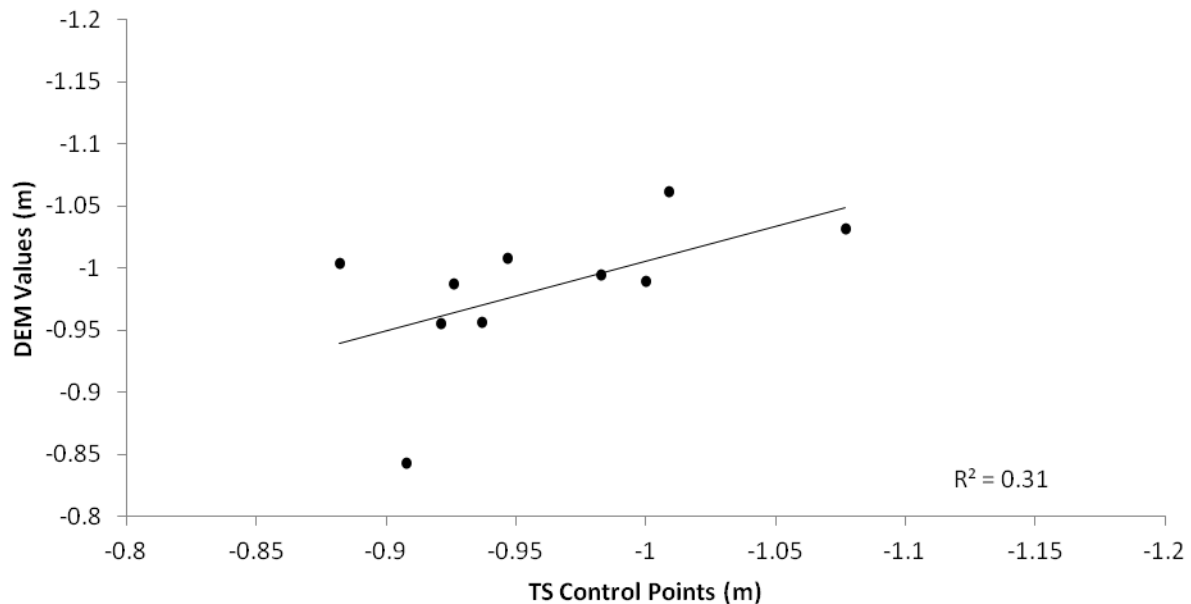


Figure 3.16: Scatter plot and simple linear regression with corresponding SFPC TS and DEM control point z values plotted against one another

3.3.2 *North Fork Peachtree Creek*

The percent differences between DEM and TS BW and BD values range from 0.6 to 31.6 and 0.6 to 20.0, respectively (Table 3-2). The linear regression for the TS and DEM control point z values shows an R^2 value 0.78, where $n = 17$ (Fig. 3.17). The standard error and the p-value are, respectively, 0.10 and <0.05 .

Table 3-2: TS and DEM BW and BD values for NFPC, as well as the percent difference between these values

Transect	Total Station (m)		SfM DEM (m)		Absolute Difference (m)		Percent Difference (%)	
	BW	BD	BW	BD	BW	BD	BW	BD
0x	21.0	2.96	15.3	2.78	5.74	0.18	31.6	6.3
1x	22.2	3.26	22.1	3.52	0.14	0.26	0.6	7.7
2x	19.2	3.55	21.4	3.36	2.20	0.19	10.8	5.5
3x	21.1	3.24	22.2	3.17	1.07	0.07	4.9	2.2
4x	21.4	3.18	22.4	3.20	0.97	0.02	4.4	0.6
5x	17.1	2.43	18.4	2.97	1.28	0.54	7.2	20.0
6x	20.6	3.24	21.3	3.11	0.70	0.13	3.3	4.1
7x	24.1	4.15	24.4	3.60	0.30	0.55	1.2	14.2
8x	23.3	3.81	22.9	3.35	0.36	0.46	1.6	12.8
9x	N/A	N/A	N/A	N/A	N/A	N/A	N/A	N/A
10x	22.0	3.60	21.6	3.56	0.42	0.04	1.9	1.1
Mean					1.3	0.2	6.8	7.5
Median					0.8	0.2	3.9	5.9
Std. Dev.					1.7	0.2	9.3	6.4

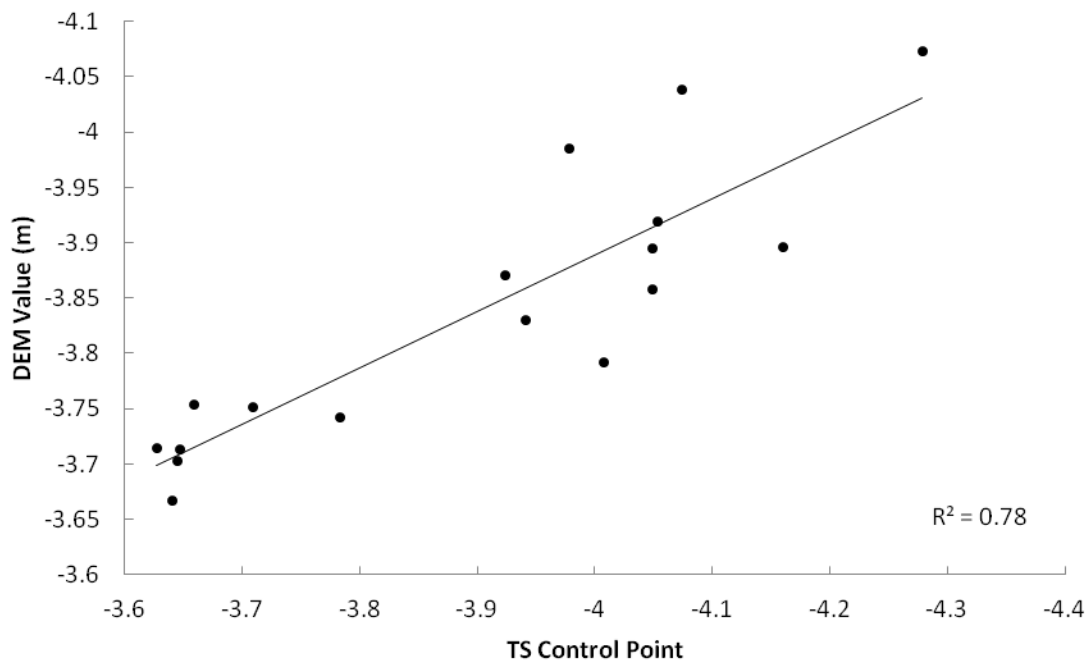


Figure 3.17: Scatter plot and simple linear regression with corresponding NFPC TS and DEM control point z values plotted against one another

4 Discussion

Although incomplete, the Proctor Creek DEM chunks and transects initially showed promise for continuing a method comparison-based research project. Due to lost data, a quantitative topographic data comparison was not possible, but because of the troubleshooting involved with the Proctor Creek group project, DEM generation for SFPC and NFPC was made significantly easier, both in the imagery collection and processing phases.

The SFPC study area was chosen as a follow up to the Proctor Creek project because SFPC did not have many of the characteristics that made data imagery collection difficult at Proctor Creek. Drone flights were considerably easier and quicker at SFPC, and 507 (out of an initial 1300+) images resulted in a DEM with a resolution of 2.76cm. A high resolution DEM is one of the supposed benefits of SfM, but unfortunately the DEM was not accurate relative to the accepted TS method. Not only were the DEM transect BW and BD values variable and, on average, significantly different from the TS transect values, but the submerged control point z values were also not strongly correlated as indicated by a low R^2 value and a high p-value (>0.05) possibly indicating that the DEM does not result in accurate submerged topography.

Unlike the SFPC study area, the NFPC site was chosen because it is similar to Proctor Creek in width and depth, and for a final study area, it seemed beneficial to, once again, attempt to overcome some of the issues involved in collecting drone-based imagery in a larger wadeable stream. Over 1,500 hundred photos were captured, and a 937 of those were used to create the model and DEM. Unlike with Proctor Creek, it was decided that it would be best to process the photos as one chunk rather than split it up into sections, which increases processing time. The resulting resolution was 2.9cm, and the BW and BD values were much less variable and not as significantly different from one another. Furthermore, the GCP values appear promising as well. With a R^2 value of 0.7* and a p-value <0.05 , there is an indication that the values are strongly correlated.

4.1 Considerations for Future Work

Because UAV-based SfM photogrammetry is an emerging method, studies using it should spend some effort focusing on the process of troubleshooting. This study, which began with the Proctor Creek study area and ended with the NFPC study area, showed progress throughout with respect to improving apparent DEM accuracy. The Proctor Creek DEM was incomplete and took a long time to process the 3 separate chunks. This was a first attempt at using a UAV and at using SfM software, but through this process it was possible to consider adjusting the methodology slightly for future work.

The first lesson learned from Proctor Creek was that while technically unnecessary, GCPs are a very important to the process. At Proctor creek, not enough were used given the size of the reach, and they were not carefully labeled and noted throughout the surveying. The GCPs reduce processing error and give the model a better reference for creating a DEM. It is also best to start with more because they may not always resolve well and may not be used for

georeferencing. Once work was started at SFPC, an effort was made to create many brightly colored GCPs (bricks for submerged GCPs) and write descriptive notes about them during surveying so that distinguishing one from another in the photos would be easier. The same was done at NFPC, in addition to bricks, Photoscan's premade targets were used as well (Fig. 3.18).

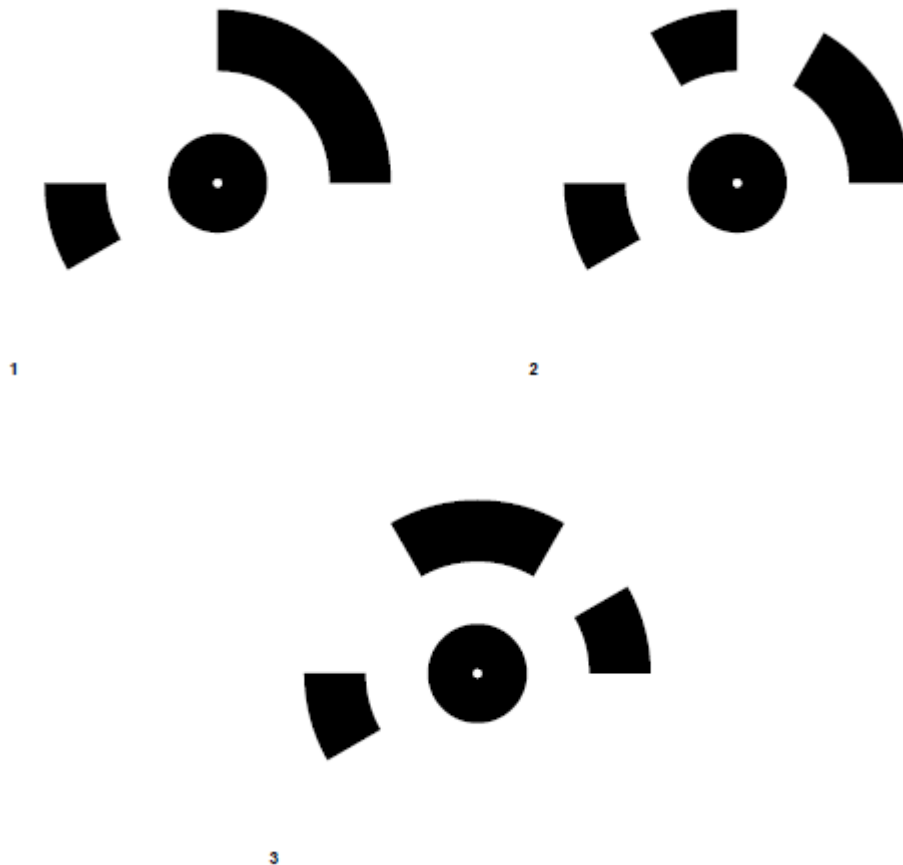


Figure 3.18: Example of Photoscan premade targets for GCP use*

The benefit of the Photoscan targets is that Photoscan automatically adds the individual points into the GCP database while also marking the locations in each photograph in which they occur. This could ultimately reduce data management and processing time significantly by

* Agisoft LLC, 2013, Agisoft PhotoScan User Manual: Professional Edition, Version 1.0.0,

http://downloads.agisoft.ru/pdf/photoscan-pro_1_0_0_en.pdf.

eliminating manual GCP selection. At NFPC, only a few were printed and used simply to test their ease of use. The targets were printed large enough to fill individual 8.5"x11" sheets of paper, and they were placed throughout the scene. Photoscan was able to automatically recognize every target but not in many photos. This was because the average flying height at NFPC had to be much higher (due to trees and area size), which made the ground resolution coarse and ultimately made it impossible for Photoscan to "see" the targets. It would have been more effective to print significantly larger targets and laminate them to use for repeat surveys.

In addition to better understanding of GCP use and placement, this study made it possible to consider better UAV flight practices. At Proctor Creek, flights simply did not provide enough coverage to resolve the entire reach. At SFPC, there was just barely enough coverage, and at NFPC there was a little bit more than was needed. However, at each site, it still would have been beneficial to acquire more imagery and from as many top-down viewpoints as necessary. As shown in this study, Photoscan produces images showing relative camera locations, which serves as a great tool to learn from so that better flight decisions can be made. The best flight pattern is one that is variable in all directions. It is important to get many low altitude images so that the ground resolution will be optimized, but the higher altitude images serve to tie more points together. At NFPC, several hundred bankside photos were taken and processed with the UAV photos, but less than 5% of these were aligned in the first attempt at a model, thus they were not used in the final model. Perhaps it is best to only use top-down photos when possible, which seems easier for Photoscan to match and reduces refraction effects.

Besides image coverage, flight practices, and GCP placement, it is also important to understand sources of error in order to approach future work. Sources of error are present in both the SfM process and TS surveying. In this study, GCP selection error may have led to less

accurate results, particularly in the case of SFPC. When selecting GCP locations, the extent of the GCP in the imagery consists of many pixels and selected point locations may vary for each GCP. The use of targets would greatly reduce this user-based error and could result in more accurate results. In addition to sources of error within the SfM process, TS surveying is also prone to user error. The majority of the error is the result of having an unlevel rod when the point values are determined by the TS. On hard surfaces this is typically easy to overcome, but on soft sediment and in dense vegetation (e.g. fluvial settings in the southeast U.S.) this may be unavoidable. Thus, although TS surveying is a widely used method, it is known to yield error in both precision and accuracy for stream surveys.

In this study, it can also be shown that site conditions can also have a significant effect on SfM model accuracy. For instance, vegetation can make it difficult to capture adequate imagery of the ground surface, resulting in a DEM that overestimates elevations. In the southeastern U.S., this is most easily overcome by surveying in the winter, late fall, and early spring. Even though this time frame is not unreasonably constrictive, it could also be said that UAV-based SfM surveying may be best suited for other conditions. As an example, braided streams in the western U.S. may be far better suited for future studies. These studies could be particularly interesting, considering some areas of braided streams change morphology more rapidly than other stream types. This is not to say studies in the southeastern U.S. are not recommended, but because this study focuses on method development, potential changes in study areas should also be mentioned to better evaluate SfM.

5 CONCLUSIONS

The purpose of this study was to evaluate the accuracy and ease of use SfM-derived fluvial topographic data in comparison to other accepted, widely-used methods, particularly total station methods. The results are mixed in that they do not consistently show the SfM DEM being accurate relative to the TS data. However, the results may show some promise for UAV-based SfM topographic data. Throughout the study, the results seem to show improvement. The NFPC was the final study area, and the DEM is significantly more accurate than the SFPC DEM. Furthermore, UAV-based SfM appears to offer a more repeatable method than total station surveying in that it is cheaper and quicker. Total station surveying took 2 full days of work at Proctor Creek and took most of the day for SFPC and NFPC. At all NFPC and SFPC, UAV surveying took less than an hour. The processing time can be lengthy, but most of it is time that does not require user interaction.

Due to variable results, this study does not determine UAV-based SfM photogrammetry to be a preferred method relative to TS surveying, but this work should suggest that further work needs to be done testing this emerging method. In addition to evaluating accuracy, this study also focused on development of new methodologies to and considerations for future studies. Thus, this study might prove useful as a guide for similar work involving UAV-based SfM photogrammetry. Furthermore, SfM technology and drone availability appear to be improving. Throughout this project, Agisoft has regularly made newer versions of Photoscan available, and each improvement made more tools available that were specific to DEM generation. Within a relatively short amount of time, UAV-based surveying has become more widely used in fields

other than fluvial geomorphology. This study has outlined some of the reasons for which UAV-based SfM surveying are problematic in this field of study, but the increasingly widespread use of these new technologies shows promise overcoming sources of error. Because this is an emerging method, there is still plenty of opportunity for improvement in methodology, possibly leading to more consistent and more accurate results.

REFERENCES

- Agisoft LLC, 2013, Agisoft PhotoScan User Manual: Professional Edition, Version 1.0.0, http://downloads.agisoft.ru/pdf/photoscan-pro_1_0_0_en.pdf.
- Bailly, J-S, Kinzel, P.J., Allouis, T., Feurer, D., and Le Coarer, Y., 2012, AirborneLiDAR methods applied to riverine environments, *in* Carbonneau, P.E., and Piegay, H., eds, *Fluvial Remote Sensing for Science and Management*: Chichester, UK, Wiley-Blackwell.
- Bailly J-S, Le Coarer, Y., Languille, P., Stigermark, C., and Allouis, T., 2010, Geostatistical estimation of bathymetric LiDAR errors on rivers: *Earth Surface Processes and Landforms*, v. 35, p. 1199–1210
- Baltsavias, E.P., 1999, Airborne laser scanning: basic relations and formulas: *ISPRS Journal of Photogrammetry & Remote Sensing*, v. 54, p. 199–214.
- Bangen, S.G., Wheaton, J.M., Bouwes, N., Jordan, C., 2014a, A methodological intercomparison of topographic survey techniques for characterizing wadeable streams and rivers: *Geomorphology*, v. 206, p. 343–361.
- Bangen, S.G., Wheaton, J.M., Bouwes, N., Jordan, C., Volk, C., Ward, M.B., 2014b, Crew variability in topographic surveys for monitoring wadeable streams: a case study from the Columbia River Basin: *Earth Surface Processes and Landforms*, v. 39, p. 2070-2084.
- Bertin, S., Friedrich, H., Delmas, P., Chan, E. Gimel'farb, G., 2015, Digital stereo photogrammetry for grain-scale monitoring of fluvial surfaces: error evaluation and workflow optimisation: *ISPRS Journal of Photogrammetry and Remote Sensing*, v. 101, p. 193–208.
- Beshr, A.A., and Elnaga, I.M.A., 2011, Investigating the accuracy of digital levels and reflectorless total stations for purposes of geodetic engineering: *Alexandria Engineering*

- Journal v. 50, p. 399–405.
- Brasington, J., Rumsby, B.T., and McVey, R.A., 2000, Monitoring and modelling morphological change in a braided gravel-bed river using high resolution GPS-based survey: *Earth Surface Processes and Landforms*, v. 25, p. 973–990.
- Carbonneau, P.E., Fonstad, M.A., Marcus, W.A., and Dugdale, S.J., 2012, Making riverscapes real: *Geomorphology*, v. 123, p. 74-86.
- Carbonneau, P.E., Lane, S.N., and Bergeron, N, 2006, Feature based image processing methods applied to bathymetric measurements from airborne remote sensing in fluvial environments: *Earth Surface Processes and Landscapes*, v. 31, p. 1413-1423.
- Clapuyt, F., Vanacker, V., and Van Oost, K., 2015, Reproducibility of UAV-based earth topography reconstructions based on Structure-from-Motion algorithms: *Geomorphology*, doi:10.1016/j.geomorph.2015.05.011.
- Dietrich, J.T., 2015, Riverscape mapping with helicopter-based Structure-from-Motion photogrammetry: *Geomorphology*, doi:10.1016/j.geomorph.2015.05.008.
- Fitzpatrick, F.A., Waite, I.R., D'Arconte, P.J., Meador, M.R., Maupin, M.A., and Gurtz, M.E., 1998, Revised methods for characterizing stream habitat in the national water-quality assessment program, *Water-Resources Investigations Report 98-4052*: U.S. Geological Survey, Raleigh, NC.
- Fonstad, M.A., Dietrich, J.T., Courville, B.C., Jensen, J.L., and Carbonneau, P.E., 2013, Topographic structure from motion: a new development in photogrammetric measurement: *Earth Surface Processes Landforms*, v. 38, p. 421–430.
- Gregory, B.M. and Calhoun, D.L., *Physical, Chemical, and Biological Responses of Streams to Increasing Watershed Urbanization in the Piedmont Ecoregion of Georgia and Alabama*,

- 2003, Scientific Investigations Report 2006–5101-B: U.S. Geological Survey, Reston, Virginia.
- Gruen, A., 2012, Development and status of image matching in photogrammetry: The Photogrammetric Record, v. 27, p. 36–57.
- Hicks, D.M., 2012, Remotely sensed topographic change in gravel river beds with flowing channels, *in* Church, M. and Biron, P., eds., Gravel-bed Rivers: Processes, Tools, Environments: Chichester, UK, Wiley-Blackwell, p. 303-314.
- James M.R. and Robson, S., 2012, Straightforward reconstruction of 3D surfaces and topography with a camera: accuracy and geoscience application: Journal of Geophysical Research v. 117, 17 p.
- Javernick, L., Brasington, J., and Caruso, B., 2014, Modelling the topography of shallow braided rivers using Structure-from-Motion photogrammetry: Geomorphology, v. 213, p.166–182.
- Kang, R.S., Storm, D.A., and Marston, R.A., 2010, Downstream effects of urbanization on Stillwater Creek, Oklahoma: Physical Geography, v. 31, p. 186-201.
- Kaufmann, P.R., Levine, P., Robison, E.G., Seeliger, C., and Peck, D.V., 1999, Quantifying Physical Habitat in Wadeable Streams, EPA/620/R-99/003: U.S. Environmental Protection Agency.
- Kinzel, P.J., Legleiter C.J., and Nelson J.M., 2013, Mapping river bathymetry with a small footprint green lidar: applications and challenges: Journal of the American Water Resources Association, v. 49, p. 183–204.
- Lane, S.N., Widdison, P.E., Thomas, R.E., Ashworth, P.J., Best J.L., Lunt I.A., Sambrook Smith G.H., and Simpson, C.J., 2010, Quantification of braided river channel change using archival

- digital image analysis: *Earth Surface Processes and Landforms*, v. 35, p. 971–985.
- Lane, S.N., and Carbonneau, P.E., 2007, High resolution remote sensing for understanding instream habitat, *in* Wood, P.J., Hannah, D.M., and Sadler, J.P., eds., *Hydroecology and Ecohydrology*: Chichester, UK, John Wiley and Sons, p. 185-204.
- Lane, S.N., James, T.D., and Crowell, M.D., 2000, Application of digital photogrammetry to complex topography for geomorphological research: *Photogrammetric Record*, v. 16, p. 793–821.
- Lejot J., Delacourt C., Piegay H., Fournier T., Tremelo, M-L, and Allemand P., 2007, Very high spatial resolution imagery for channel bathymetry and topography from an unmanned mapping controlled platform: *Earth Surface Processes and Landforms*, v.32, p. 1705–1725.
- Marcus, W.A., Fornstad, M.A., and Legleiter, C.J., 2012, Management applications of optical remote sensing in the active river channel, *in* Carbonneau, P.E.and Piegay, H., eds., *Fluvial Remote Sensing for Science and Management*: Chichester, UK, Wiley-Blackwell, p. 19-42.
- Marcus, W.A., and Fonstad. M.A., 2007, Optical remote mapping of rivers at sub-meter resolutions and watershed extents: *Earth Surface Processes and Landforms*, v. 33, p. 4–24.
- Mertes, L.A.K., 2002, Remote sensing of riverine landscapes: *Freshwater Biology*, v. 47, p. 799–816.
- NOAA Office for Coastal Management, 2010, Digital Coast Data Viewer: coast.noaa.gov/dataviewer (accessed October 2015).
- Ouédraogo, M.M., Degré, A., Debouche, C., and Lisein, J., 2014, The evaluation of unmanned aerial system-based photogrammetry and terrestrial laser scanning to generate DEMs of

- agricultural watersheds: *Geomorphology*, v. 214, p. 339-355.
- Price, K., and Leigh, D.S., 2006, Morphological and sedimentological responses of streams to human impact in the southern Blue Ridge Mountains, USA: *Geomorphology*, v.78, p. 142–160.
- Snavely, N., Seitz, S.M., and Szeliski, R., 2007, Modeling the world from internet photo collections: *International Journal of Computer Vision*, doi: 10.1007/s11263-007-3.
- Turner, D., Lucieer, A., and Wallace, L., 2015, Direct georeferencing of ultrahigh-resolution UAV imagery: *IEEE Transactions on Geoscience and Remote Sensing*, doi: 10.1109/TGRS.2013.2265295 (in press).
- Vallé, B.L., and Pasternack, G.B., 2006, Field mapping and digital elevation modeling of submerged and unsubmerged hydraulic jump regions in a bedrock step–pool channel: *Earth Surface Processes and Landforms*, v. 31, p. 646–664.
- Wehr, A., and Lohr, U., 1999, Airborne laser scanning—an introduction and overview: *ISPRS Journal of Photogrammetry & Remote Sensing*, v. 54, p. 68–82.
- Westoby, M.J., Brasington, J., Glasser, M.J., and Hambrey M.J., and Reynolds J.M., 2012, Structure-from-Motion photogrammetry: a low cost, effective tool for geoscience applications: *Geomorphology*, v. 179, p. 300–314.
- Wheaton, J.M., Brasington, J., Darby, S.E., and Sear, D.A., 2010, Accounting for uncertainty in DEMs from repeat topographic surveys: improved sediment budgets: *Earth Surface Processes and Landforms*, v. 35, p. 136-156.
- Woodget, A.S., Carbonneau, P.E., Visser, F. and Maddock, I.P., 2014, Quantifying submerged fluvial topography using hyperspatial resolution UAS imagery and structure from motion photogrammetry: *Earth Surface Processes and Landforms*, v. 40, p. 47-64.